AFFDL-TR-78-176

TEMPERATURE BASED STRESS ANALYSIS OF NOTCHED MEMBERS

B. I. SANDOR

E. H. JORDAN

UNIVERSITY OF WISCONSIN-MADISON
750 UNIVERSITY AVENUE
MADISON, WI 53706

MARCH 1979

Final Report - AFOSR 77-3194 September 1976 - February 1979

AIR FORCE FLIGHT DYNAMICS LABORATORY
AIR FORCE WRIGHT AERONAUTICAL LABORATORIES
AIR FORCE SYSTEMS COMMAND
WRIGHT-PATTERSON AIR FORCE BASE, OHIO 45433

NOTICE

When Government drawings, specifications, or other data are used for any purpose other than in connection with a definitely related Government procurement operation, the United States Government thereby incurs no responsibility nor any obligation whatsoever; and the fact that the government may have formulated, furnished, or in any way supplied the said drawings, specifications, or other data, is not to be regarded by implication or otherwise as in any manner licensing the holder or any other person or corporation, or conveying any rights or permission to manufacture, use, or sell any patented invention that may in any way be related thereto.

This report has been reviewed by the Information Office (OI) and is releasable to the National Technical Information Service (NTIS). At NTIS, it will be available to the general public, including foreign nations.

This technical report has been reviewed and is approved for publication.

Gene E. Maddux

GENE E. MADDUX
Project Engineer

Nelson D. Wolf

NELSON D. WOLF, Acting Chief
Structural Integrity Branch
Structures & Dynamics Division

FOR THE COMMANDER

Ralph L. Kuster, Jr.

RALPH L. KUSTER, JR., Col, USAF
Chief, Structures & Dynamics Division

If your address has changed, if you wish to be removed from our mailing list, or if the addressee is no longer employed by your organization please notify AFFDL/FBE, WPAFB, OH 45433 to help us maintain a current mailing list.

Copies of this report should not be returned unless return is required by security considerations, contractual obligations, or notice on a specific document.

UNCLASSIFIED

SECURITY CLASSIFICATION OF THIS PAGE *(When Data Entered)*

REPORT DOCUMENTATION PAGE		READ INSTRUCTIONS BEFORE COMPLETING FORM
1. REPORT NUMBER AFFDL-TR-78-176	2. GOVT ACCESSION NO.	3. RECIPIENT'S CATALOG NUMBER
4. TITLE *(and Subtitle)* TEMPERATURE BASED STRESS ANALYSIS OF NOTCHED MEMBERS		5. TYPE OF REPORT & PERIOD COVERED Final Report Sep 76 to Feb 79 6. PERFORMING ORG. REPORT NUMBER
7. AUTHOR(s) B. Sandor E. Jordan		8. CONTRACT OR GRANT NUMBER(s) AFOSR 77-3194
9. PERFORMING ORGANIZATION NAME AND ADDRESS University of Wisconsin 750 University Avenue Madison, WI 53706		10. PROGRAM ELEMENT, PROJECT, TASK AREA & WORK UNIT NUMBERS Project 2307 Task N1 Work Unit 04
11. CONTROLLING OFFICE NAME AND ADDRESS Air Force Flight Dynamics Laboratory (AFFDL/FBE) Wright-Patterson AFB, Ohio 45433		12. REPORT DATE December 1978 13. NUMBER OF PAGES
14. MONITORING AGENCY NAME & ADDRESS*(if different from Controlling Office)*		15. SECURITY CLASS. *(of this report)* Unclassified 15a. DECLASSIFICATION/DOWNGRADING SCHEDULE

16. DISTRIBUTION STATEMENT *(of this Report)*

Approved for public release; distribution unlimited.

17. DISTRIBUTION STATEMENT *(of the abstract entered in Block 20, if different from Report)*

18. SUPPLEMENTARY NOTES

19. KEY WORDS *(Continue on reverse side if necessary and identify by block number)*

experimental stress analysis
temperature measurement
plastic zone size
plasticity
residual stress
thermocouples

20. ABSTRACT *(Continue on reverse side if necessary and identify by block number)*

The purpose of this effort was to develop and demonstrate a method of experimentally determining both elastic and plastic strain distributions in metallic materials. This was accomplished by recording minute temperature changes on the surface of the material as it was subjected to various loading conditions. Mathematical relationships relating these changes to the strain in the material was developed and verified. Much of the success of this effort was due to the development of thermocouple attachment and readout technique that recorded minute temperature changes (0.1 degree centigrade) at ten millisecond sample

DD FORM 1 JAN 73 1473 EDITION OF 1 NOV 65 IS OBSOLETE

UNCLASSIFIED

SECURITY CLASSIFICATION OF THIS PAGE *(When Data Entered)*

intervals. This small time period sampling assures that heat has not been conducted away from the thermocouple attachment point. The thermocouples consisting of two .13 mm dissimilar metal wires were attached to the surface 0.1 mm apart by discharging a large capacitor grounded to the specimen. The small size permits the mounting of several thermocouples in a small area. The determination of plastic zone outlines is thereby facilitated.

ABSTRACT

The purpose of this effort was to develop and demonstrate a method of experimentally determining both elastic and plastic strain distributions in metallic materials. This was accomplished by recording minute temperature changes on the surface of the material as it was subjected to various loading conditions. Mathematical relationships relating these changes to the strain in the material was developed and verified. Much of the success of this effort was due to the development of thermocouple attachment and readout technique that recorded minute temperature changes (0.1 degree centigrade) at ten millisecond sample intervals. This small time period sampling assures that heat has not been conducted away from the thermocouple attachment point. The thermocouples consisting of two .13 mm dissimilar metal wires were attached to the surface 0.1 mm apart by discharging a large capacitor grounded to the specimen. The small size permits the mounting of several thermocouples in a small area. The determination of plastic zone outlines is thereby facilitated.

TABLE OF CONTENTS

LIST OF FIGURES

LIST OF TABLES

SECTION I

INTRODUCTION

The purpose of this project was to demonstrate that the use of temperature data in stress analysis of metallic members gives information that is both valid and useful. Work is presented to specifically:

1. Demonstrate the feasibility by developing a system capable of measuring the desired temperatures.
2. Demonstrate the validity of interpreting temperature data by developing and testing an equation relating mechanical variables to measure temperature change developed.
3. Demonstrate the usefulness of the technique through two example applications.
    a. The use of temperature measurement to determine plastic zone size.
    b. The use of temperature measurement to detect time dependent relaxation of overload produced residual stresses in notched members.

The stress analysis technique developed is one of perhaps thirty experimental stress analysis techniques already available. Therefore, it is important to consider why an additional technique is valuable. First, it is worthwhile to consider what information one would ideally like to obtain in experimental stress analysis. In the most general case one would like to know the six components of the stress tensor field, six components of the elastic strain tensor field and six components of the plastic strain tensor field. In addition, it is usually desirable to have this information in real time by a nondestructive method at a low cost. No existing technique can even come close to meeting these requirements. As a result, the choice of a technique is dictated by the features deemed most important for a particular application.

The technique that has been developed is an important addition to the available techniques because of the

features which it combines. The technique developed has the chief advantages of being non-destructive, giving real time information, being relatively low in cost, distinguishing elastic from plastic deformation, and most importantly providing quantitative information.

This technique is applicable to a wide range of problems, the full extent of which cannot be immediately foreseen. However, the advantages of this technique make it particularly suited to the study of notched members. To see why this is so, it is necessary to consider the nature of the experimental problem which must be faced in the study of notched members.

In smooth centroidally loaded members it is possible to calculate stress from load. However, the vast majority of service failures involve notched members. Unfortunately, it is not possible to calculate stress from load alone in such members. It is also nearly impossible to measure stress experimentally. Without the ability to measure stress it is not possible to use the stress-strain curve in distinguishing plastic and elastic strain as is commonly done for unnotched members. The inability to measure stress and distinguish elastic from plastic strain is the key problem in studying notched members.

Many different experimental methods have been devised to attack this problem. One measure of the importance of this problem is the large number of techniques devised or employed in dealing with it. Some of these techniques are as follows: x-ray microbeam,[1] chemical etching,[2] microhardness,[3] image-distortion,[4] transmission electron microscopy,[5] holographic interferometry,[6] photoelastic coating,[7] selected area electron channeling,[8] reference mark methods,[9] Moire interference techniques,[10] and exoelectron methods.[11] In spite of the large number of techniques available, investigators will often find it necessary to compromise between desirable and undesirable attributes. It is the present technique's ability to distinguish plastic from elastic deformation in real time nondestructively that makes it a good choice for the study of the mechanical behavior of notched members.

1.1 HISTORY OF TEMPERATURE MEASUREMENT IN DEFORMATION BEHAVIOR

The basics of temperature response of deforming metals were established before the end of the nineteenth century. There are two major temperature effects that occur. One associated with elastic deformation and one associated with plastic deformation.

During elastic deformation there is either cooling or heating due to volume change. The temperature change associated with elastic deformation was studied by Thompson and in 1851 he proposed an equation which is the equivalent of Eq. (1).[12] This equation states that temperature is linearly related to volume dilatation.

The second major temperature effect in deforming metals is heating associated with plastic deformation. There is evidence that blacksmiths knew about and used this fact for hundreds and perhaps thousands of years before scientists studied it.[13] In 1875 Hirn published experimental results that showed that when a metal is plastically deformed all the irreversible work is converted to heat.[14] Much of the subsequent work on fundamental temperature effects in metals is concerned with the small fraction of irreversible work that is not converted to heat.

Microstructural Applications

The first and most extensive use of temperature measurement in the study of deformation of metals was in the study of stored energy of cold work. Extensive review papers have been published dealing with this subject so it will only be discussed briefly here.[15,16]

The main purpose of studying stored energy of cold work is to increase the understanding of the microstructural changes associated with plastic deformation. There are two common ways of studying stored energy of cold work. Both methods involve temperature measurement.

Several investigators have measured highly localized temperatures as a means of studying the micromechanisms of energy dissipation.[17,18,19] In one of these studies[17] special attention is paid to the nonhomogeneity of plastic deformation. This investigator pioneered the use of highly sophisticated infrared temperature measurement techniques. Progress has been made in identifying the mechanisms of energy dissipation in metals, however, no definitive results have emerged.

Mechanics Applications

Temperature measurement has been used by O. W. Dillon and coworkers in studies of both linear and non-linear thermoelasticity.[20-24] Theoretical work by Dillon showed that non-linear elasticic materials would dissipate mechanical energy as heat due to coupling effects between the temperature field and the deviatoric components of strain.[20]

An extensive experimental program was carried out. The results of experiments on both tubular and solid cylindrical torsion specimens showed that the heat generation as a function of strain did not agree with that predicted by non-linear thermoelasticity. These experiments produced three additional findings particularly relevant to this thesis. First, the rate of heat generation at some places within a cycle was not equal to the rate at which irreversible mechanical work was done.[24] This first finding contradicts experimental findings in this thesis. Second, in spite of the fact that creep was observed for static loading the heat generation was frequency independent.[22] Third, generation of heat by mechanical deformation in aluminum was not sensitive to prior load history.[23]

For the study of linear thermoelasticity, Dillon developed an impressive thermocouple based temperature measurement system capable of measuring very small temperatures dynamically.[24] For electrical reasons the system was inherently limited to a single channel because the difficult problem of an electrically insulating but thermally conducting interface was not solved. This system was used to check temperature changes predicted by thermoelasticity. The experimental results were in

excellent agreement with the theoretical results of thermoelasticity.

V. A. Franyuk and V. B. Rantsevitch used temperature measurement to determine the plastic work during fatigue tests.[25] In these experiments the temperature rise in unnotched fatigue specimens cycled at a constant frequency was measured as a function of time. By also recording stress-strain hysteresis loops the temperature change which had major contributions from thermal conduction was correlated with the plastic work done. Temperature measurement was then used as a substitute for determining hysteresis loop areas.

D. G. Montgomery has developed a method of determining fracture toughness by integrating the measured temperature differences near the running crack during fracture.[26] The toughness values measured in this way were correlated with toughness determined by other methods. It is claimed that the method can easily determine toughness in members with complex geometry.

K. Schonert and R. Weichert have measured temperatures near a fast running crack and claim that their data implies temperatures as large as 1000 K to 2000 K.[27,28] Such large temperatures would have implications for the choice of appropriate models of fast running cracks.

A. D. Abdi et al have developed a promising system of measuring temperatures in deforming metals based on the use of thermistor flakes.[27] The system was used to show that more heating occurs near stress concentrations.

The most extensive use of temperature measurement in mechanics has thus far been in the identification of areas of fatigue damage in steady state fatigue cycling. This is accomplished by using infrared field temperature measurement techniques to identify hot spots associated with areas of greatest ongoing fatigue damage. The earliest reference found to this is that of R. Attermo and G. Ostberg.[30] However, many others[31-34] have done extensive work in the area, especially K. Reifsnider.[31] In all of these investigations the temperature distribution of specimens during continuing fatigue cycling was monitored. From the observed temperature distribution these investigators were able to identify sites of maximum fatigue damage rate, detect fatigue cracks, watch them propagate and identify the site of final fracture. In all tests to date, continuous fatigue cycling was used, resulting in quasi-steady state temperature distribution which is the result of a balance between conduction and heat generation. Because the effects of conduction are

included in the temperature data collected it is not possible to quantitatively relate temperature at any point to mechanical variables.

The present investigation should be considered a mechanics application of temperature measurement during mechanical deformation. The important features of this work are that it develops a quantitative stress analysis technique applied to difficult problems associated with notched members. The key element that makes these applications of temperature data possible is rapid loading combined with rapid data collection. Without this element of speed the data would be changed by thermal conduction making quantitative interpretation impossible.

SECTION II

EXPERIMENTAL SET UP

The experiments for this project were carried out using two similar mild steels. The material used for the majority of the experiments was a commercially available 14 gage (t=1.95 mm) hot rolled low carbon steel sheet containing not more than 0.15% C, 0.6% Mn, 0.35% P, and 0.04% S. This material was heat treated in a variety of ways before testing. Table 1 lists the heat treatments and the results of all tensile tests. It is apparent from Table 1 and from tests of notched specimens that there is no significant difference between the mechanical properties of heat treatments six through nine. In the remainder of this thesis heat treatments six through nine will be referred to as simply heat treated mild steel. To distinguish heat treatment five from the others this heat treatment will be referred to by number.

Four different specimen geometries were used in tests involving this material; large unnotched rectangular plates 400 mm x 76 mm x 1.95 mm inserted 76 mm into grips at each end, small rectangular plates 200 mm x 25 mm x 1.95 mm inserted about 50 mm into grips at each end, large rectangular specimens with a single edge notch (see Fig. 1 for the notch geometry), and large rectangular specimens

with a 15 mm diameter center hole (Fig. 2). The edge notch and center hole specimens were identical to the large rectangular specimens except for the addition of either a notch or a hole. The elastic stress concentration for the notched specimen was 5.1[35] while for the plate with the 15 mm center hole the stress concentration was 2.51.[36]

For reasons discussed later, it became necessary to test cylindrical specimens. Cylindrical specimens of the material used for the other tests were not readily available so specimens of a similar low carbon steel (Type A 36, single specimen yield strength = 589 MPa) were used. These specimens were threaded with a smooth section 65 mm long and 5 mm in diameter.

Heat treatment was done using existing electrical resistance furnaces. Excussive formation of mill scale and possible decarbonization was avoided by covering the specimens with cast iron chips during most high temperature heat treatments. A tube furnace for inert gas heat treatment was used for some tests. This furnace has a proportional controller and provisions for using an argon atmosphere during heat treatment.

A load cell was used to measure forces. With the exception of residual stress measurement by hole drilling all strains were measured with 25 mm gage length strain gage extensometers. In some experiments extensometers were mounted on opposite narrow sides of the specimens and the output was averaged using a differential amplifier. In the hole drilling experiments metal foil strain gages were used.

In some cases it was desirable to test the thin plate specimens in compression. In order to prevent buckling special grips and anti-buckling plates were constructed (see Fig. 3). The validity of stress-strain data obtained with this type of anti-buckling plates has been established by others.[37]

The most difficult experimental problem was measuring small, rapidly changing temperatures. Generally in this work it was necessary to measure temperatures as small as a few tenths of degrees Celcius with a response time of a hundredth of a second or better. The system chosen to accomplish this is based on thermocouples. Thermocouple systems do not give field data as do some infrared systems,

but they have certain advantages and are far less expensive. The key element in making a thermocouple system of sufficiently fast response is intimate thermal contact between the measuring junction and the specimen. A variety of thermocouple attachment methods have been used successfully.[24-27,38] In this work individual thermocouples were welded to the specimen surface. This particular attachment method is quite suitable for stress analysis for the following reasons. It is relatively nondestructive and nondisturbing of stress fields, allows precise positioning of the measuring junctions, allows the position of the measuring junction to be freely observed throughout the test, and provides excellent thermal contact. This system can also be expanded for using as many thermocouples as needed.

The thermocouple consisted of 0.127 mm diameter copper and constantan or chromel and constantan wires welded directly to the specimen. The reference junction of these thermocouples is an air reference junction located on a solder tab glued to the specimen (see Fig. 4). A small amount of slow drift results from using an air reference junction. This causes no major problems because the temperature that is related to mechanical deformation changes extremely rapidly compared to the rate of drift. Welding of the thermocouple to the specimen was accomplished by touching each thermocouple wire individually to the specimen and short circuiting a 2500 μF capacitor charged to 20 V. Additional information on the thermocouple system and the procedure used to install the thermocouples is given in Appendices Ia and Ib.

The output of the thermocouples in these experiments was a microvolt size signal which was amplified and recorded. To accomplish this each thermocouple was connected to its own 10^5 gain differential amplifier. The output of the amplifier was then recorded using a light pen oscillograph or digital storage oscilloscope. A more detailed description of how the electronics were handled to reduce noise may be found in Appendix II.

Experiments were performed to estimate the response time of the thermocouple system. Temperature change due to elastic deformation should be in phase and linearly related to load changes. To test the response time fast rising load pulses were applied to an unnotched specimen. The resulting temperature and load data were examined for evidence of delay of the temperature response with respect to the applied load. No delay was detected for a 0.01 s rise time load pulse which is the fastest pulse that the testing machine could produce. The response time of the system could not be determined. These experiments did however demonstrate that the response time of the system is less than 0.01 s.

In all the experiments performed in this investigation, data were sought that were not significantly influenced by conduction. The influence of conduction was detected by noticing whether or not the temperatures changed when the rate of loading was increased. Conduction was considered eliminated when an increased loading rate no longer changed the observed temperatures. For the unnotched specimens, the lowest allowable frequency (sine wave) for which conduction was negligible was 0.2Hz. For the notched specimens and specimens with center holes, a load with a rise time of 0.04 or less was found to be the slowest

allowable rise time to eliminate significant conduction during loading. All the data in this report was collected from tests performed at rates high enough to eliminate significant contributions due to conduction.

SECTION III

THE RELATIONSHIP BETWEEN MECHANICAL VARIABLES AND TEMPERATURE CHANGE

Quantitative temperature based stress analysis is achieved by relating measured temperatures to mechanical variables through an equation which is based on known physics.[12,16] The derivation and experimental verification of an equation suitable for this purpose will be discussed in this section. An alternate derivation of a similar equation is possible based on general thermodynamics.[23] The derivation presented is designed to provide a basis for understanding subsequent discussions, and to emphasize the assumptions involved. Experimental verification of the equation is important for two reasons. First, in measuring the small transient temperatures many misleading signals can be recorded (see Appendix II). Correlation of measured temperature with temperature predicted by thermoelasticity theory provides excellent proof that temperatures are indeed being measured. Others have experimentally demonstrated that thermoelasticity theory accurately predicts temperature change for elastic deformation.[24] Second, for inelastic deformation the assumptions used in deriving the equation may be violated to greater or lesser degrees depending on the material used, plastic strain amplitude, and mode of deformation.[16]

It is therefore important to verify the accuracy of the equation for each new material for the strain range and mode of deformation anticipated.

3.1 DERIVATION OF THE EQUATION

Temperature changes occurring in mechanically deforming metals can be thought of as being the result of three different effects; heating or cooling resulting from volume change associated with elastic deformation, heating associated with plastic deformation, and thermal conduction.

Purely Elastic Deformation

In 1851 Lord Kelvin[12] proposed the following equation which describes the temperature change associated with elastic deformation.

$$\Delta\theta = - \frac{3\theta\alpha K e}{\rho c} \qquad (1)$$

where

$\Delta\theta_e$ = change in absolute temperature from elastic effects

θ = absolute temperature

α = coefficient of thermal expansion

K = bulk modulus

e = volume dilatation

c = specific heat

ρ = mass density

This equation is based on the equations of classical elasticity and classical thermodynamics and therefore should be very accurate. This equation predicts temperature decrease for tensile normal stress increments and temperature increase for compressive normal stress increments.

Purely Plastic Deformation

In the following discussion four assumptions are used.

1. Strain may be separated into an elastic part and a plastic part.

$$E_t = E_p + E_e$$

where

E_t = small strain tensor, total strain

E_e = small strain tensor, elastic strain

E_p = small strain tensor, plastic strain

2. Plastic deformation occurs in an incompressible manner.

$$e_p = 0$$

where

e_p = plastic volume dilatation

using

$$e_e = KP$$

and the first assumption,

$$e = e_p - KP = -KP$$

where

P = pressure

e_e = elastic dilatation

3. All plastic work is converted to heat.

4. The small strain assumption of classical elasticity holds.

Numerous experiments have shown[15,16,38] that usually considerably more than 90 percent of plastic work is converted to heat. Applying the third and fourth assumptions above the temperature change due to plastic deformation is given by:

$$\Delta\theta = \oint \frac{T:dE_p}{\rho c} \quad \text{... for uniaxial loading}$$

$$= \left\{ \frac{\text{hysteresis loop area}}{\text{specific heat/unit volume}} \right\} \tag{2}$$

where

$\Delta\theta_p$ = change in absolute temperature from plastic effects

T = Cauchy stress tensor

Case of Combined Elastic and Plastic Deformation with Conduction

The equation describing conduction in the presence of heat sources is the following:

$$\nabla^2\theta + \frac{q}{k} = \frac{1}{D}\frac{d\theta}{dt} \tag{3a}$$

where

∇^2 = Laplacian operator

q = time rate of heat generation per unit volume

k = thermal conductivity

D = thermal diffusivity = $\frac{k}{\rho c}$

t = time

If a system undergoes a state change from an initial to a final state, the temperature change can be found by integrating the above equation. The resulting equation is:

$$\Delta\theta = \theta_2 - \theta_1 = \frac{q}{\rho c} + D \int_{t_1}^{t_2} \nabla^2\theta dt \qquad (3b)$$

where

q = heat generated during the state change.

Subscripts 1 and 2 will be used in this equation and throughout this report to designate the values of variables in the initial and final states, respectively.

The thermal effects of plastic and elastic deformation may be superimposed and treated as heat sources as follows:

$$q = \rho c(\Delta\theta_e + \Delta\theta_p) \qquad (4)$$

The equation describing temperature change during combined plastic and elastic deformation is obtained by putting Eq. (1) and Eq. (2) into Eq. (4) and then Eq. (4) into Eq. (3), resulting in:

$$\Delta\theta = D \int_{t_1}^{t_2} \Delta^2\theta dt + \oint \frac{T dE_p}{\rho c} - \frac{3K\theta\alpha}{\rho c}\Big|_{e_1}^{e_2} e \qquad (5a)$$

Using assumption 2, the above equation can also be written as:

$$\Delta\theta = D \int_{t_1}^{t_2} \nabla^2\theta dt + \oint \frac{T dE_p}{\rho c} \quad \frac{3\theta\alpha}{\rho c}\Big|_{p_1}^{p_2} P \qquad (5b)$$

These two forms of Eq. (5) are the equations that will be used to describe temperature change during elastic and plastic deformation of metals.

There are two important implications of the above equations. First, the conduction term is not directly related to any mechanical variables and as such its contribution to temperature change must be eliminated in order to draw valid conclusions about the values of mechanical variables implied by temperature change. Second, it can be shown that any stress-strain path beginning and ending at the same stress will have no net temperature change contributed by elastic deformation. This second point provides one way of distinguishing plastic and elastic deformation.

3.2 EXPERIMENTAL VERIFICATION OF THE EQUATION

In all experiments in this section loading rates were sufficiently high that temperature change by conduction was negligible.

Verifying Equation (5) for Adiabetic Elastic Deformation

Four unnotched specimens were used for this series of tests. These specimens were subjected to square wave, triangular wave, and haversine wave loading in the elastic range at frequencies ranging from 1 Hz to 25 Hz. From each loading, plots of temperature vs. time, load vs. strain were obtained. A typical example of the data generated in this set of experiments is shown in Fig. 5.

For the case of uniaxial adiabatic elastic deformation, the terms for conduction and plasticity are dropped and Eq. (5b) becomes:

$$\Delta\theta = \frac{\theta\alpha\sigma}{c\rho} \tag{6}$$

where

σ = normal stress

It is apparent in Fig. 5 that the general shapes of the load vs. time plot and the temperature vs. time plot are the same, as the linear form of Eq. (6) implies they should

be. Consistent with Eq. (6), Fig. 5 shows that a load cycle beginning and ending at the same load results in a temperature cycle beginning and ending at the same temperature.

A comparison of experimental results with results predicted using Eq. (6) is shown in Fig. 5. The solid line in Fig. 6 is Eq. (6), while the dotted line is a line fit to the data by least squares. The slopes of the two lines are the same within six percent.

The size of the scatter band in Fig. 6 is very nearly equal to the noise level on temperature shown in Fig. 5. In conclusion, Eq. (5) is verified for adiabatic elastic deformation within experimental error. This agreement with thermoelasticity theory which is known to be accurate[24] is important because it shows that the temperature measurement system is functioning as intended.

Verifying Equation (5) for Adiabatic Plastic Deformation

The same specimens and wave forms were used in this set of experiments that were used in the previous set except that frequencies were kept below 5 Hz in order not to exceed the frequency limit of the extensometers used. The net temperature change was measured in adiabatic load cycles beginning and ending at the same load level. For a uniaxial load cycle under these conditions the conduction term and thermoelastic term are zero and Eq. (5b) becomes:

$$\Delta\theta_{net} = \oint \frac{\sigma d\varepsilon_p}{c} = \frac{\text{hysteresis loop area}}{\text{specific heat/unit volume}} \qquad (7)$$

where

$\Delta\theta_{net}$ = net temperature change

ε_p = axial plastic strain

A comparison of experimental results with results predicted using Eq. (7) is shown in Fig. 7. The solid line in Fig. 7 is Eq. (7), while the dotted line was fit to the data by the least squares method. The slopes of the two lines agree within twelve percent.

Examples of data from this set of experiments are shown in Fig. 8 and Fig. 9. The general shape of the curves in Fig. 8 and Fig. 9 can be explained using Eq. (5b) and the fact that mild steel has a nearly flat topped stress-strain curve. In accordance with Eq. (5b), the two figures exhibit linear temperature decrease with increasing tensile stress, temperature increasing with little increase in load during nonstrain hardening plastic deformation, and temperature increasing linearly with decreasing load on elastic unloading. It is worth noting that the slopes of the elastic portions of Fig. 9 are within six percent of the values predicted using Eq. (1).

Verifying Equation (5) for Reversed Cyclic Loading

Experiments were performed using cylindrical A37 low carbon steel specimens 65 mm long and 5 mm in diameter. Cylindrical specimens were used in these tests because they are easier to load in compression than are the thin plates used in all other experiments. If thin plates were to be used for reversed loading it would be necessary to use guide plates to prevent buckling. Guide plates would add the potential complication of heating due to rubbing of the guide plates on the specimen. Using cylindrical specimens the stress-strain curve was recorded simultaneously with the temperature change. Using Eq. (5) and the measured stress-strain curve, the temperature change was predicted. A typical example of the data collected in these experiments is shown in Fig. 10. In this figure the temperature predictions of Eq. (5) and the measured temperature are in good agreement.

This series of experiments shows that Eq. (5) is not only valid for predicting temperature change from elastic deformation alone or plastic deformation alone but also that Eq. (5) is valid for predicting temperature change when elastic and plastic deformation occur simultaneously.

In summary, Eqs. (5a), and (5b) predict the general shape and give reasonable quantitative values for the temperature changes occurring during mechanical deformation.

SECTION IV

METHODS FOR SEPARATING ELASTIC FROM PLASTIC DEFORMATION

In this section immediate advantage is taken of the availability of the equations relating temperature change and mechanical variables to analyze possible methods of distinguishing elastic and plastic strains. The equations developed in this report make possible the explicit identification of assumptions necessary for distinguishing plastic and elastic strains, and the quantitative estimation of some of the limitations of various special methods. This section also includes data illustrating the use of at least one special case of each of the three proposed methods. The major emphasis is in demonstrating those techniques that the author will apply to notched specimens.

Measurements of the scalar quantity temperature change provides quantitative values of one or more combinations of the following four scalars: dilatation rate, magnitude of dilatation, specific plastic work, and rate of specific plastic work.

Three different methods of distinguishing elastic and plastic deformation are being proposed. For convenience, the methods are referred to as follows: the round trip method, the sign method and the magnitude method. In discussing these three methods, adiabatic conditions will be assumed.

4.1 THE ROUND TRIP METHOD

Restriction: The stress cycle must begin and end with the same value of the pressure:

$$P = -\frac{1}{3}(\sigma_1 + \sigma_2 + \sigma_3)$$

In any loading conforming to this restriction, the net temperature change defined in Fig. 11 is equal to the specific plastic work divided by the specific heat per unit volume. This can be shown by discarding the conduction term from Eq. (5b). Under this restriction, the result is an equation identical to Eq. (2). This method therefore provides the following information:

(1) it makes possible the determination of whether or not plastic deformation occurred, and

(2) it gives a quantitative value of specific plastic work using Eq. (7).

The ability to determine specific plastic work has already been given in Fig. 3. In addition, the ability to detect the occurrence of plastic deformation as in Item (1) above appears to be excellent. In these experiments, net heating was detected for plastic strains as small as 0.0003.

4.2 THE SIGN METHOD

Restriction: The value of $\frac{dP}{dt}$ is less than zero (i.e., normal stresses are becoming more tensile).

Under the above restriction, the sign of temperature change from elastic deformation is negative while plastic deformation always produces heating. This sign difference provides a basis for distinguishing one from the other.

Case 1: Ideally elastic plastic material (flat top yielding) - The application of Eq. (5a) shows that for an ideally elastic plastic material the temperature vs. time plot has a minimum which occurs when yielding first occurs. Because of the minimum point, the pre- and postyield temperature change can be distinguished. In the material being discussed, the pre-yield behavior is entirely elastic and the temperature change is given by Eq. (1). The postyield behavior of such a material is mainly plastic and the temperature change is given by Eq. (2). It is therefore possible to obtain the following information:

(1) the volume dilatation at any point during the elastic portion of the deformation, using Eqs. (5b) and (5c):

$$e = -\frac{\Delta\theta c\rho}{3\alpha K\theta}, \quad \text{or} \quad \frac{1}{3}(\sigma_1 + \sigma_2 + \sigma_3) = -P = \frac{\Delta\theta\rho c}{3\alpha\theta}$$

(2) the instant at which yielding occurs which corresponds to the minimum point on the temperature vs. time plot;

(3) the specific plastic work at any time after yielding which may be determined using Eq. (2).

The determination of these three items can be demonstrated experimentally using part of the data used in verifying Eq. (2). The data chosen for this experimental demonstration is limited in two ways. First, plastic strains must exceed 0.002 in order to produce a clear sign change. Second, the load must go from zero to maximum in less than 2 s but more than 0.2 s to avoid drift and electrical noise problems. For uniaxial deformation, volume change is proportional to normal stress. It is possible to verify Item (1) (volume dilatation) by comparing stress change determined from temperature measurement (value A in Fig. 11) with stress determined from load cell data. In Table 2 temperature determined stress is compared to load cell determined stress. Also shown is the percent error resulting from using temperature to determine stress. In computing the error, load cell determined stress was assumed to be the correct stress. The average error magnitude is six percent.

Item (2) (yielding) may be investigated by determining the smallest plastic strain that can be consistently and

unambiguously detected by the sign method. In these experiments, plastic strains as small as 0.002 could be detected.

To experimentally verify Item (3), the specific plastic work was determined by measuring the temperature change following the minimum point up until the point where the maximum load was reached (value B in Fig. 11). In Table 3, specific plastic work values determined from these measured temperatures are compared to specific plastic work values determined from stress-strain data. Also shown are the error percentages of these values. The average error is eleven percent. In every case the temperature method results in an underestimation of the value of specific plastic work. In summary, these experiments demonstrate that within certain limits of accuracy and resolution the sign method is capable of providing the above described three kinds of information.

Case 2: power law strain hardening material - The stress-strain behavior of the majority of metals under cyclic loading can be described by the following stress-strain relation.

$$\varepsilon = \frac{\sigma}{E} + \left[\frac{\sigma}{k'}\right]^{1/n'} \qquad (8)$$

n' = cyclic strain hardening exponent

k' = cyclic strength coefficient

E = the elastic modulus

The upper portion of Fig. 10 is a graphical representation of this type of stress-strain relation. Eq. (8) is also a good approximation for the monotonic stress-strain behavior of some materials. Because power law strain hardening is so common it is worthwhile to consider the implications of such behavior to the use of the sign method. In materials exhibiting stress-strain behavior of the type shown in Fig. 11 strain increments consist of both elastic and plastic components. At lower stress, elastic strain makes up the major part of the strain increments while at higher stresses plastic strain makes up an increasingly larger fraction of the strain increment. The time-temperature behavior for such a material when undergoing tensile loading has a minimum point. The minimum point is preceded by decreasing temperature resulting from the dominance of elastic effects and followed by increasing temperature resulting from the dominance of plastic effects. For such a material two methods of distinguishing elastic and plastic deformation are possible depending on how much is known about the stress-strain behavior.

The first situation is where the exact equation of the stress-strain behavior is known as well as the starting values of stress and strain. In this situation it would be possible to calculate the stress-strain path and get the components of elastic and plastic strain. The accuracy is limited only by the accuracy of Eq. (5) and by the accuracy of the assumed stress-strain relation. In the experiments of this report this approach was not used. An idea of the accuracy that could be attained with this method is gotten by considering the accuracy with which Eq. (5) predicted the temperature changes in Fig. 10.

The second situation is where nothing is known about the stress-strain relation of the metal being studied. In this case the stress-strain behavior can be assumed to be ideally elastic-plastic. The values of mechanical variables determined would of course be approximate. For materials for which the constants in Eq. (5) and Eq. (8) are known these two equations can be used in conjunction to calculate the resulting error and also to calculate the smallest detectable plastic strain. In Appendix III the equations giving the smallest detectable plastic strain (Ep) the error in estimating the stress present when the temperature minimum is encountered (El)

and the error in estimating the plastic strain (E2) are derived utilizing Eq. (5) and Eq. (8). Numerical values of these quantities are calculated for several common metals. The materials constants for these metals are given in Table 4. The smallest detectable plastic strains which are those existing when the time temperature curve is at a minimum are given in the first column of Table 5. In the second column of this table the percent error in estimating the stress present at the minimum point on the time temperature plot is given. The third column of Table 5 gives the expected error if the temperature increase following the minimum is used to estimate the plastic strain level for the case where the member has experienced tensile plastic strain of one percent. The values in the bottom row of the table are experimentally determined values from the experiments described in section 3.2. In calculating the errors from the experimental values the measured stress and strain are treated as correct.

The data in Table 5 indicates that the error resulting from assuming ideally elastic-plastic stress-strain behavior for a power law strain hardening material are small enough to give useful approximate information.

4.3 THE MAGNITUDE METHOD

Restriction: The maximum temperature increase due to elastic effects cannot exceed some prescribed value.

In this method, the net temperature change is recorded at the completion of a cycle or cycles, and any temperatures above a threshold temperature are interpreted as being from plastic deformation. The choice of a reasonable threshold temperature depends upon what is assumed about the deformation being studied. The round trip method is a special case of the magnitude method. It is worth mentioning two other examples.

The first example is the case where continuous fatigue cycling is applied. In such a case a quasi-steady state temperature distribution develops. Conceptually, if cycling is rapid enough, even small amounts of irreversible deformation could result in temperature changes large enough for positive identification as irreversible deformation. As was the case with previous methods, this method has certain limitations. One limitation is that analysis of quasi-steady state data precludes observations of short term transient phenomena. A second and more important limitation is the lack of a mathematically unique relationship between magnitude and spatial

distribution of temperature change and the magnitude and spatial distribution of plastic deformation due to the effects of conduction. However, this method has the advantage of generating comparatively large temperature changes. The usefulness of this method has been clearly demonstrated elsewhere.[31-33]

A second kind of magnitude method is based on the fact that for any real material there is an upper limit to the size of temperature increase that can be caused by elastic effects in a single cycle of loading. The size of the largest possible temperature increase can be estimated from Eq. (1) if a yield criterion is assumed. The assumptions of such a temperature estimation are made conservatively enough to assure that the limiting temperature can only imply plastic deformation. The uniaxial experiments performed in the present investigation suggest that a reasonable limit temperature for mild steel is 1 C which corresponds to a plastic strain of about 0.01. In the case of multiaxial deformation, the correct failure theory combined with knowledge of the stress state would have to be used to estimate the maximum temperature change due to elastic deformation. Several failure theories for general three dimensional stress states admit the possibility of an infinite threshold temperature.

In summary, this magnitude method cannot detect plastic strains as small as the method previously discussed and in the worst case detects no plastic strain. However, the restrictions on the conditions for which this method may be used are less severe than for any other method and in some cases may represent a reasonable approach to distinguishing elastic and plastic deformations.

SECTION V

PLASTIC ZONE SIZE BASED ON TEMPERATURE DATA

The methods to measure temperature and interpret such measurements in terms of mechanical variables were developed in preceding sections. The usefulness of temperature based stress analysis will now be explored. In this section the use of temperature measurement for the determination of plastic zone size will be discussed.

The determination of plastic zone size is important in fracture mechanics to the equivalent crack length concept, to defining the amount of plastic deformation allowable in problems validly treated by linear elastic fracture mechanics, and in understanding crack propagation retardation by overload. A. Kfouri and K. Miller suggest that plastic zone sizes play a decisive role in nonlinear fracture mechanics.[40] In addition, the measurement of plastic zone size could be used to check the accuracy of plasticity theory or finite elements solutions to elastic-plastic notch problems.

The determination of plastic zone size from temperature data will be based on the methods of separating elastic from plastic deformation developed in Chapter 4. This method of determining plastic zone size was considered worth developing because it is a

real time method, non destructive, comparitively inexpensive, applicable to nearly all metals, usable for both monotonic and cyclic zones and does not require the use of an assumed failure theory.

As was previously discussed, methods of separating plastic from elastic deformation involve assumptions. Because of the possible uncertainty introduced by using these assumptions this section is mainly concerned with attempts to compare plastic zone sizes determined by temperature measurement with plastic zones determined by other methods. Both experimental and theoretical methods are used for comparison. This chapter also discusses measurements of large components of postyield time dependent deformation which happened to be measured while running the validation experiments for this section.

5.1 TECHNIQUES FOR USING TEMPERATURE DATA TO DETERMINE ZONE SIZES

Plastic zone size may be determined by applying any of the three previously discussed methods of separating plastic from elastic strain to a series of locations in an area where a plastic zone is expected. The plastic zone is considered to extend over the area for which non-zero

values of plastic work are detected. In this report only the round trip and the sign method will be used. Before applying these methods to the determination of plastic zone size it is important to consider their validity for the deformation field near a notch.

In the round trip method it is assumed that in a complete load cycle the hydrostatic stress is the same before and after the cycle. In notched members undergoing local plastic deformation the residual stress state is likely to change significantly when the load is first applied or whenever the cyclic load amplitude changes. Clearly, if the residual stress state changes during a load cycle the assumption upon which the round trip method is based can not be used. For this reason, the use of the round trip method for the first cycle of loading or for load cycles following load amplitude changes is not recommended. During constant amplitude cycling the residual stress levels change slowly if at all. The sign method can be used for plastic zone size determination for constant amplitude loading. Furthermore, for power law strain hardening behavior typical of cyclic loading the round trip method can detect much smaller plastic strains than the sign method (see Chapter 4).

Valid use of the sign method requires that the pressure be increasing monotonically. During the loading portion of the load cycle this can only fail to happen if there is local unloading due to load redistribution. Unloading causes heating that would be mistaken for plastic deformation. Unloading therefore only gives unrealistic plastic zone sizes if the region that is experiencing unloading has not already yielded. Unloading in elastically deforming regions is unlikely except near the zone edge.[41] Unloading near the zone edge will result in overestimation of the plastic zone size. This overestimation is part of the inherent error of this method. It is expected that the error from this cause will not be very large. However, this error is one of the chief reasons that this method should be verified using other methods.

Figure 12 shows data from both the round trip method (net heating) and the sign method (heating from tensile plastic flow) plotted as a function of distance from the notch root along the minimum cross section. The specimen used had a single edge notch of the geometry shown in Figure 1. Ten cycles of load giving a nominal stress in the minimum cross section equal to 0.7 times yield stress were applied. The solid line shows the temperature

response on the first cycle and the dotted line shows the response on the tenth cycle. Non-zero values of the plotted temperatures indicate plastic deformation. The plastic zone edge is taken to be wherever the temperature change drops to zero. Several features in this figure are worth noting. First, both the amount of heating and the plastic zone size are much larger on the first cycle than on the tenth. This difference is the basis for the methods used in the assessment of residual stress in subsequent chapters. Analitical solutions predicting a difference between the first and all subsequent cycles will be discussed in section 6.1 while experimental measurements of this difference are described in reference 8. Second, the plastic zone size based on net heating data is significantly larger than that based on heating from tensile plastic flow. Arguments presented in the preceding section showed that the use of net heating data to determine first cycle plastic zone size was not completely valid. The difference between the more correct plastic zone size based on the heating form tensile plastic flow data and the zone size based on net heating data suggest that the errors from using net heating data on the first cycle are significant. Finally, the plastic zone size for the tenth cycle is similar for both types

of data as would be expected from two methods that both should be valid for this type of zone.

In summary, the sign method should be used for the first cycle of loading or whenever cyclic amplitude is changing because the round trip method is of questionable validity in such cases. The superior sensitivity of the round trip method can be taken advantage of for constant amplitude cyclic loading.

5.2 PLASTIC ZONE SIZES BASED ON TEMPERATURE DATA AND OTHER METHODS

Temperature based plastic zone size determination involves several assumptions. It is therefore desirable to compare the plastic zone sizes determined from temperature data with plastic zone sizes determined by other methods. Unfortunately, none of the attempts to do this were completely successful. However during these investigations, valuable insight into some of the limitations of the temperature based method was gained and unexpectedly large amounts of postyield time dependent deformation were recorded. The following description of the difficulties encountered in trying to measure plastic zone size by other methods is an excellent indication of the need for a new technique for determining plastic zone size such as temperature based stress analysis.

There are two general classes of methods for determining plastic zone size; methods based on measuring total strain and methods based on measuring some physical quantity directly connected with the physical process of plastic deformation. Examples of the former are strain gage methods, photoelastic coating and holography. Examples of the latter are exoelectron emission, chemical etching and microhardness. Strain based methods involve the use of assumed failure theories which creates certain problems as will be discussed later. In an attempt to avoid failure theories two non-strain based methods were tried, microhardness and chemical etching.

Plastic deformation of annealed metals usually results in an increase in hardness due to work hardening. Several experimenters have measured hardness as a function of distance from a stress concentration and detected hardness profiles which indicate the extent of the plastic zone.[3,42,43]

Several notched specimens were given different heat treatments designed to soften the mat material. It was hoped that these heat treatments would excentuate the difference between the hardness of the cold worked zone and the surrounding material. In spite of these heat treatments and careful mechanical polishing no variation in hardness near the notch was detected. There are several possible reasons for the failure to detect plastic zones by this method.

1. Mild steel does not work harden at the strain levels encountered.
2. Polishing work hardens the surface uniformly thus masking the plastic zone profile. Electro-polishing could perhaps eliminate this problem.

The second attempt to determine plastic zone size was through the use of Fry's reagent which has been shown to turn plastic zones black in mild steel.[2,44,45,46] The method is based on the increase in dislocation density which occurs during plastic deformation. After straining, the mild steel is aged at room temperature or higher to get nitrogen to diffuse to the dislocations. The presence of nitrogen on the dislocations makes areas of high dislocation density subject to chemical action which blackens those areas. A dozen or so edge notched specimens were mechanically tested and their plastic zone size estimated

using temperature based stress analysis. The notch root section of each specimen was cut out and subjected to a variety of postdeformation aging procedures ranging from 15 minutes at 250 C to 6 months at room temperature. The notch root sections were mounted in plastic, polished to the .05 micron alumina stage and etched in Fry's reagent. Out of 12 specimens tested, only the three aged six months at room temperature etched so as to reveal their plastic zone. The zones revealed were extremely narrow (a few mm) and two to three times as long as indicated by temperature based stress analysis. It was also noticed that before polishing and under oblique light the plastic zone could be seen as a slightly depressed area on the surface of the specimen. The zone size and shape seen under oblique lighting was very similar to that revealed by etching.

Clearly, the etching and oblique lighting results were in sharp disagreement with the results of temperature based stress analysis. Two reasons for this disagreement were apparent. First, the thermocouples were located on a line centered at the notch which was perpendicular to the edge of the specimens while many of the zones were not centered exactly at the notch root. The thermocouples in many cases missed the zone. Second, under oblique lighting it could be seen that the zone in many cases was made up not of an area of plastic deformation but of narrow lines of plastic deformation presumed to be Luders bands. These

lines nearly always missed the thermocouples. In addition, the rate of conduction away from such a thin (1 mm or less) heated zone would be extremely rapid, perhaps rapid enough to make the zones undetectable.

In summary, the etching method turned out to be unreliable for the mild steel studied. Two specimens treated in nominally identical manners will not necessarily both etch properly. In addition, 6 months of room temperature aging is excessive for practical reasons. The etching results do conclusively show, however, that for long thin zones consisting of individual deformation bands, the temperature based determination of zone sizes using only four thermocouples was not successful. To handle such zones one would require an extremely fast field temperature measurement technique.

5.3 PLASTIC ZONE SIZES BASED ON TEMPERATURE DATA AND COMPUTER SOLUTION

This section compares the monotonic plastic zone size determined from temperature based stress analysis with a computer solution based on the elastic stress distribution. The elastic stress distribution used is that of an elasticity solution by Howland.[36] The computer

solution is based on ideal elastic plastic stress-strain behavior (flat topped) and takes into account the redistribution of stress caused by yielding.

The preceding non-strain based experiments were not successful partly because the edge notched specimens had zones of a shape that temperature based stress analysis could not handle very well. In an attempt to avoid this problem the remaining experiments of this section were run using rectangular specimens with single circular center holes (see Fig. 1). This specimens geometry was selected for several reasons. First, a theoretical solution for the elastic stress distribution of this geometry is known.[36] The elastic stress distribution can be used to estimate plastic zone size and provide a comparison for temperature based determinations. Second, the zone expected based on the elastic stress distribution is fairly wide which will help to avoid the problem of the plastic zone missing the thermocouples. It was also hoped that a wider zone would be less likely to form as isolated Luder bands.

The diameter of the circular center hole was chosen to be exactly one-fifth of the width of the plate so that the elasticity solution could be used without having to interpolate for any of the coefficients involved.[36] All specimens were tested with four thermocouples mounted along the minimum cross section. The location of the thermocouples was chosen so as to best detect a plastic zone of the size expected for each particular test.

A simple solution based on the elastic stress distribution is obtained by defining the zone edge to be those points in the elastic stress distribution where the criterion for yielding is just reached. Such an approach results in the stress distribution ACD of Fig. 13. In this simple solution the equilibrium in the axial direction is violated by an amount proportional to area ABC in Fig. 13. The solution developed in this report is based on an iterative procedure which redistributes this load. There is no unique manner in which this load can be redistributed. In this work the load is redistributed so that in addition to satisfying equilibrium, the assumed stress distribution beyond the edge of the plastic zone is given by the elasticity solution with the nominal stress suitably adjusted so that

equilibrium is satisfied. The effect of considering the redistribution of load is shown in Fig. 14 where the plastic zone size based on maximum shear stress theory is plotted vs. the applied stress divided by the yield stress. The solid line is the solution which takes account of the load redistribution while the broken line ignores load redistribution. It is clear from the figure that for larger zone sizes the two solutions are quite different.

In Fig. 15 two computer solutions that both account for load redistribution are compared with the results of temperature based stress analysis. One of the two solutions is based on maximum shear stress theory while the other is based on octahedral shear stress theory. Temperature based stress analysis was interpreted using the sign method and resulted in determination of the plastic zone edge as lying between two thermocouples. It is worth pointing out that with temperature measurement at a few additional locations it would be possible to extrapolate the temperature data to the zero temperature change location and determine the plastic zone size much more precisely. In Fig. 16 the vertical bars indicate the range of possible zone sizes determined by temperature based stress analysis. The figure shows that for zones

larger than 3 mm the temperature determined plastic zone sizes agree with the zone sizes predicted by octahedral shear stress theory and are slightly less in some cases than the zone sizes predicted by maximum shear stress theory. The smallest zone determined from temperature data is smaller than that predicted by either theory. In light of the fact that there is scatter in the yield strength of this material and the theoretical solution is approximate, the data in the figure supports the contention that the temperature determined zone sizes are approximately correct. The lack of agreement at the smallest zone size suggests but does not prove that for a specimen loaded to .6 of minimal yield there is either not enough plastic strain to produce easily measured temperature increase or that conduction is so rapid away from the zone that the full size of the zone is not detected.

SECTION VI

TIME DEPENDENT RELAXATION OF RESIDUAL STRESSES IN NOTCHED MEMBERS

In the preceding sections evidence supporting the feasibility and validity of temperature based stress analysis was presented along with the results of attempts to use the method for the determination of plastic zone size. The purpose of this chapter is to demonstrate that temperature data can also be used to ascess the degree of stress relief in notched members.

When a notched member is loaded to a stress high enough to produce local plastic deformation residual stresses are produced in the region of the notch. Tensile overloads are known to produce compressive residual stresses while compressive overloads are known to produce tensile residual stresses.

The problem being studied in this section will be limited to time dependent relaxation of residual stresses in overloaded members with finite root radius notches. The study of stress relaxation in members with finite width notches should provide insight into the residual stress effects in "infinitely sharp" propagating fatigue cracks. However, to avoid confusion it is important to

make a distinction between the problem of sharp fatigue cracks and the finite width notches being investigated in this report.

The main significance of compressive residual stresses produced by tensile overload is in the fatigue of notched members. A notched member subjected to a large tensile load and subsequently cycled at a lower load level will exhibit an extended fatigue life.[47-51] Typically, the fatigue life may be extended by a factor of three to five. The effect of a tensile overload on fatigue can be subdivided into two major effects.

First, any large strain cycle will produce a certain amount of damage of its own. It has been demonstrated that a single large cycle when no residual stresses are present causes an amount of damage exceeding that which would be expected from the Palmgrem-Miner linear damage rule.[52] It has been suggested that this is so because overload initiates cracks that can be propagated at lower stresses.[52]

Second, tensile overloads produce compressive residual stresses which act to lower the mean stress of the subsequent smaller load cycles.

It has long been known that lower mean stresses result in longer fatigue lives. There is considerable

experimental evidence that residual stresses effect fatigue lives in a manner explainable in terms of mean stress effects.[53] It is apparent from the fact that tensile overloads lengthen the fatigue life of notched members that the mean stress effects are more important than the damaging effect associated with the overload itself.

The picture just presented of the effect of overload has been deliberately simplified in order to establish the basic situation. Compressive residual stresses are not always permanent. There are two major causes for their relaxation, one of which the present investigation considers in detail.

Residual stresses can be relaxed by the action of repeated plastic straining in a process called cyclic dependent relaxation.[48] Because of this relaxation, the effect on fatigue-life of multiple overloads is often much greater than single overloads.[48] Multiple overloads continuously reintroduce the residual stresses that cyclic plasticity remove. The occurrence of cycle dependent relaxation of residual stresses depends on the plastic strain amplitude in a manner which is still a subject of controversy.[48,54] It can be said, however, that the extent

to which this phenomenon occurs varies greatly from case to case depending on plastic strain amplitude and is not always a major consideration.

Residual stresses can also be removed by heating in a process called stress relief. Many engineering structures are subjected to temperatures for which various degrees of stress relief occur. Because of the effect of residual stresses on fatigue life it is important to know whether or not such stress relief is taking place.

Several investigators have studied the possibility of time dependent relaxation of overload produced residual stresses. In the investigation of aluminum two different investigators failed to show any relaxation effect from room temperature rest periods.[55,56] In contrast to these results Simkins and Neulieb showed considerable evidence of time dependent relaxation of residual stresses at room temperature when compressive loads were applied during rest periods.[57] The most dramatic evidence of residual stress relaxation is in the investigation of Imag.[51] In this investigation titanium was stress relieved at temperatures between room temperature and 290 C for periods between 20 s. and 30 days. These tests showed that at high temperatures the beneficial effect of tensile overload was reduced but not entirely eliminated by the annealing.

Photomicrographs showing microstructure were employed to attempt to show that the heating did not affect the microstructure. All of these investigators used change in fatigue life to assess the effect of overloads and annealing.

Before discussing the present study of stress relief it is important to recognize that in attempting to stress relieve a metal by heating a host of mechanical and metallurgical property changes may take place. Property changes caused by heating form the basis of the heat treatment of metals, which is one of the cornerstones of modern metallurgical practice. Stress relief heat treatments are often carried out at temperatures low enough that basic property changes may be small. However, it cannot be depended upon that an arbitrary stress relief heat treatment will not effect any properties other than the residual stress level. As a result of possible compound effects from stress relief heat treatments it is important to conduct experiments in such a way that the various effects of stress relief can be separated.

The lack of apparent change in microstructure is not always sufficient to prove the absence of change in mechanical behavior. In an experiment of Sandor's using unnotched mild steel specimens, fatigue lives were

extended by a factor of 100 and the yield stresses raised with no observable miscrostructural changes.[58]

The assessment of residual stress level by temperature based monitoring of notch root stress-strain behavior is a total departure from the usual method. Compared to using fatigue life as a measure of residual stress level it has the advantages of using only one specimen to evaluate several stress relaxation heat treatments and without requiring lengthy fatigue life tests.

6.1 THEORETICAL BASIS FOR ASSESSING RESIDUAL STRESSES USING TEMPERATURE DATA

It was pointed out in the section on plastic zone size determination that the notch root stress-strain response of the first cycle is very different from that of subsequent cycles. Both the plastic zone size and the plastic strain amplitudes are larger on the first cycle compared to all other cycles. The assessment of the residual stress state using temperature data exploits this difference. Specifically, this assessment is based on the following assertion:

> The difference in near notch stress-strain response between the first and all subsequent cycles is largely due to the residual stresses produced by the first cycle. A good measure of the degree of stress relief is the degree to which the first cycle notch root stress-strain response is restored by a given stress relief heat treatment.

For the above statement to be true the following assumption must hold.

> The stress-strain response of the material following stress relief must be approximately that of the virgin material.

The mild steel used in this investigation obeys this assumption particularly well in that heat treatments at temperatures as low as 150 C are sufficient to restore the sharp yield characteristic of the virgin material.

The near notch root stress-strain response was assessed by examining the two temperature quantities, the heating from tensile plastic flow and the net heating (see Fig. 11). When other variables are held constant these two temperature quantities are monotonically increasing with plastic strain amplitude. Exceptions to this will be discussed later. To provide a theoretical basis for the correlation of the two temperature quantities with residual stress level it is sufficient to show that the near notch root plastic strain amplitude is a monotonically decreasing function of compressive residual stress level. This monotonic dependence cannot be easily shown for a completely general case. However, examination of several specific solutions for the cyclic plastic deformation of cracked members lends much credence to this notion which is certainly strongly supported by physical intuition.

Residual stress does not appear explicitly in the existing solution for cyclic notch root strain amplitude. In order to use these solutions to understand residual stress effects it is necessary to establish a relationship between variables explicitly appearing in these solutions

and residual stress. The following few paragraphs will establish a relationship between effective yield strength and residual stress. Once this relationship is established it will be possible to examine expressions for plastic strain amplitude and determine the effect of residual stress change by noting the effect of changes in yield strength.

Three solutions for crack tip plastic deformation will be examined.[59,60] The relationship between residual stress and yield strength in these solutions can be understood by examining some of the details of these solutions. All three solutions follow the general scheme shown below.

$$\varepsilon_1 = f\ (P, \sigma_y, \text{Geometric terms})$$

$$\varepsilon_2 = \varepsilon_1 - f\ (\Delta P,\ 2\sigma_y, \text{Geometric terms})$$

$$\Delta\varepsilon = \varepsilon_2 - \varepsilon_1 = f\ (\Delta P,\ 2\sigma_y, \text{Geometric terms})$$

where

ε_1 = Strain for the loading portion of the first cycle

ε_2 = Strain for the unloading portion of the first cycle

$\Delta\varepsilon$ = Strain amplitude for unloading part of first cycle and all subsequent cycles

ΔP = Amplitude of load change

It is apparent from the above that for pulsating tension ($R = 0$) where $\Delta P = P$ the difference between the near notch root strain amplitude on the first application of load and on subsequent cycles is due solely to the fact that in calculating all cycles other than the first the yield stress is doubled.

The reason for doubling the yield strength can most easily be understood by considering the case of reloading after at least one previous load cycle. There exists at this point in the load history a compressive residual stress field near the notch root. In general, the stress excursion necessary to yield a material starting from a compressive stress is greater than when starting from a zero state of stress. In the theoretical solutions under consideration the material was assumed to be an ideally elastic-plastic material with the same yield strength in compression as in tension. For this material behavior the notch root residual stress at the end of the unloading cycle will be equal to the compressive yield stress. The stress excursion to yield the material in tension upon reloading is therefore equal to twice the yield strength. Generalizing from these solutions, the difference in notch root response between the first and

all other cycles is due to the residual stress state's effect on the stress excursion necessary to produce yielding upon reloading. If residual stress is removed while all other variables are left unchanged the effective yield strength upon reloading will be decreased by an amount exactly equal to the amount of residual stress removed. The effect of a change in residual stress levels can be determined from theoretical solutions by determining the effect of a change in the stress excursion necessary to produce yielding. For ideally elastic-plastic stress-strain behavior, a change in the stress excursion necessary to produce yielding is the same as a change in the yield strength.

The solutions of three different notch root geometries were examined to determine the effect of decreasing the yield strength on near notch root plastic strain amplitude. The effect of yield strength reduction was just shown to be related to the effect of stress relief. Two of the geometries examined were solved by Rice.[59] These geometries were an infinite plate with a finite center crack in simple tension and a semi-infinite plate with an edge notch opened by a wedge load. The third geometry examined was solved by Hult and McClintock.[60] This problem consisted of a very shallow circumferential notch

in a torsional member. Rice's solution utilizes rigid, fully plastic stress-strain behavior in the notch region while Hult and McClintock use linear elastic, fully plastic stress-strain behavior throughout the member. Rice's solutions involve solving a specially posed elasticity problem while Hult and McClintock have solved a problem combining an elasticity solution and classical plasticity. Rice's solution gives a quantity which is a direct measure of plastic strain amplitude while the solution of Hult and McClintock gives the value of the total strain. The total strain in Hult and McClintock's solution can easily be related to the plastic strain. The total strain is equal to the plastic strain. The total strain is equal to the plastic strain plus a constant. In spite of the differences between these solution methods all three geometries yield a solution for the notch root plastic strain in which the strain amplitude monotonically increases as yield strength decreases. It is worth noting that in Rice's solutions the increase in plastic strain amplitude is not merely monotonic but also linear with decreases in yield strength.

The solutions just discussed are based on idealized stress-strain behavior for geometries different from the geometry tested in this thesis. In spite of the differences

the qualitative notions reflected in these solutions should be applicable to the notched members studied in this thesis. These solutions are presented to show that the idea that notch root strain amplitude increases with decrease in residual stress level is supported by available theoretical results.

The correlation of residual stress level with notch root heating depends on notch root heating monotonically increasing with decreasing residual stress level. Notch root heating increases monotonically with plastic strain amplitude for most situations. The monotonic increase in plastic strain amplitude with the decrease in residual stress suggests that the correlation will be successful. There are certain complications to these arguments being used to justify this correlation that should be considered. An important limitation on the applicability of this correlation will become apparent when these complications are considered.

There is a net temperature change associated with the thermoelastic term in Eq. (5) whenever residual stresses are created. This is due to the fact that the stress undergoes a net change in its value during such a cycle. This elastic effect will increase the net heating when compressive residual stresses are created and decrease the net heating when tensile residual stresses

are created. The experiments in this chapter involve the removal of compressive residual stresses and subsequent reintroduction of the stresses upon reloading. The elastic effect from the reintroduction of compressive residual stresses increases the net heating for that cycle. The monotonic increase in net heating with the decrease in residual stress is preserved for this case. The removal and reintroduction of tensile residual stresses would have the opposite effect and could upset the monotonic increase of net heating with decrease in residual stress level. The use of net temperature change data is therefore not recommended for the study of the relief of tensile residual stresses.

Most metals exhibit strain hardening path dependent stress-strain behavior under repeated loading. No theoretical solutions for repeated loading of notched members made of such materials were found. However, a solution for the monotonic loading of power law strain hardening material is available.[61] This solution shows that for power law strain hardening the notch root strain amplitude increases as yield strength decreases. This result suggests that for a complete cycle the desired monotonic increase in notch root strain amplitude with decreasing residual stress will hold for strain hardening materials.

In summary, the detection of residual stress relief in notched members is based on a correlation between notch root heating and residual stress level. For the correlation to be good the notch root heating must change monotonically with residual stress level. The interpretation of theoretical solutions for cyclic stress-strain behavior of cracked members supports the contention that the relationship is monotonic. Consideration of various complications suggests that temperature based assessment of the degree of stress relief in the case of tensile residual stresses may not be valid. Temperature based assessment of stress relief is therefore recommended only for the case of compressive residual stresses.

6.2 EXPERIMENTS AND RESULTS

The purpose of this experimental program was to demonstrate the validity of the proposed method of assessing the degree of stress relief. In the experiments of this section either edge notched or unnotched large rectangular specimens were tested. As was discussed in the preceding section it

was desirable to minimize any mechanical property changes caused by the stress relief heat treatments. To help accomplish this all specimens used in this section were given an initial heat treatment at a temperature higher than the highest temperature used in subsequent stress relief experiments (650 C). It was hoped that the initial heat treatment would promote any changes that were likely to occur in the mechanical properties before the stress relief experimental program began.

A square wave load pulse with a hold time of 0.1 s and a rise time of 0.02 s was used in all tests of this section. The load amplitude in most tests was sufficient to produce a nominal stress in the minimum cross section equal to 70% of the nominal yield strength. A few tests were run with the stress equal to 68% of the nominal yield stress. In all tests of notched members the notch root response as indicated by temperature did not change after three cycles. The tenth cycle response was used

as representative of the cyclic notch root response throughout this report.

The procedure in assessing residual stress from temperature data is as follows. Each specimen was subjected to ten cycles of square wave loading. The temperature response at the notch root and at several other locations along the minimum cross section was recorded during the first, third, and tenth cycle. This data characterized the virgin specimen behavior. Following this testing the specimen was subjected to some sort of stress relief heat treatment. The post stress relief mechanical behavior was then determined by a ten cycle mechanical test identical to the one used before heat treatment. The degree to which an edge notched specimen notch root stress-strain response was restored to that of a virgin specimen was determined from temperature data taken on the first cycle following heat treatment. The degree of restoration was used as a measure of the degree of stress relief.

There was considerable variation in the first cycle temperature response of different specimens. In order to compare the degree of restoration of different specimens the degree to which the virgin specimen response restored was computed as a percentage. For convenience, this percentage will be referred to as the percent restoration. The percent restoration is defined below.

$$PR = \frac{\Delta T_{1S} - \Delta T_{10S}}{\Delta T_{1V} - \Delta T_{10V}}$$

where

PR = Percent restoration

ΔT_{1V} = A temperature change parameter measured on the first cycle for the virgin specimen

ΔT_{10V} = A temperature change parameter measured on the tenth cycle of loading of the virgin specimen

ΔT_{1S} = A temperature change parameter measured on the first cycle following stress relief

ΔT_{10S} = A temperature change parameter measured on the tenth cycle following stress relief

The same temperature change parameter was used when calculating any given value of percent restoration. Percent restoration was calculated for either net heating or the heating from tensile plastic flow, both

defined in Fig. 11. The percent restoration was defined in such a way as to partially compensate for changes in mechanical properties. For example, any stress relief heat treatment that strengthened the material would make both ΔT_{S1} and ΔT_{S10} smaller but would have a lesser effect on their difference which appears in the definition. The tenth cycle response of the virgin specimen and the specimen after heat treatment are in general nearly equal which indicates little change in mechanical properties due to heat treatment.

The validity of using temperature to monitor residual stress levels will be supported in two ways. First, all arguments for the uniqueness of the correlation of residual stress and temperature are based on an assumption that the heat treatments used do not substantially change the mechanical properties of the specimens. This assumption was checked experimentally. Second, the correlation of residual stress level with measured temperature response of the notch root was directly shown by correlating residual stress levels determined by hole drilling methods with the measured temperature response.

Experiments to Verify that Stress Relief Heat Treatments do not Change Mechanical Properties

The primary means normally used to determine the effect of heat treatment on the stress-strain behavior[15] is monitoring of the stress-strain behavior, both before and after heat treatment. Unfortunately, there is no easy way to directly measure stress in the vicinity of the notch root. The best that can be done is to measure the stress-strain behavior of a companion unnotched specimen subjected to the same strain history as the notch root and assume that its behavior is a good approximation of the behavior of the notch root. Usually the strain in the companion and notched specimen are matched using strain gage data. The use of strain gages at large (> .5%) strain ranges requires extensive, questionable calibration procedures.[62] In the tests carried out here the strain history was matched using notch root temperature data.

A 400 mm x 76 mm x 1.95 mm unnotched specimen from heat treatment 6 was subjected to reversed cyclic loading designed to simulate the stress-strain history at the notch root of the specimens used in the stress relaxation experiments. To simulate the fully reversed loading that occurs in the notch root guide plates (see Fig. 3) must be used to prevent buckling during compressive loading.

The stress-strain histories were matched by approximately matching the temperature vs. time behavior of the unnotched specimen to the notch root. After cycling, the specimen was subjected to a one hour heat treatment at 650 C and then cycled again. The first cycle stress-strain response of the specimen showed that the discontinuous yield behavior destroyed by cycling was restored by the heat treatment (see Fig. 16). The stress-strain hysteresis loop shapes before and after heat treatment were very nearly identical. This specimen was subjected to a second heat treatment of one hour at 150 C and tested monotonically. Again, even after 150 C heat treatment the sharp yield behavior was restored. The monotonic yield strength did not appear to be dramatically affected; being 312 Mpa for the virgin specimen, 305 Mpa after 650 C heat treatment and 338 Mpa after the 150 C heat treatment. It is apparent that the only mechanical property change produced by the heat treatment was an increase in the yield strength following 150 C heat treatment. This increase may not be valid in terms of notch root behavior because by this time the unnotched specimen had accumulated a net elongation of 8 percent which is probably not possible for a notch root region surrounded by the bulk of the specimen which is behaving elastically. This unrealistically large strain would be likely to work harden the specimen and produce an unrealistic rise in

the yield strength. However, even without dismissing this increase in yield strength there was no change in mechanical properties sufficiently large to explain the nearly three fold increase in notch root heating following complete stress relief. Furthermore, the mechanical changes observed were increases in yield strength which would produce a decrease, not an increase, in the notch root heating. This change is the opposite of what is observed, indicating that the dominant effect of the heat treatment used is not explainable in terms of mechanical property changes and therefore must be due to the effect of the removal of residual stresses as claimed.

Metallography was also used to help guard against property changes caused by heat treatment. The chief reason for employing this technique in addition to the companion specimen method was that it is far less time consuming and therefore more suitable for routine use. The notch root sections of most specimens used in the study of stress relief were examined using optical metallographic techniques. Specifically, a Nital etchant was used to reveal microstructure. Before the experimental program was started experiments were done to determine at what temperature obvious microstructural changes took place so that all tests could be done below this temperature.

It was found that above 680 C the material recrystallized from its original grain size ASTM 8 ($2048/mm^2$) to a grain size of ASTM 0 ($8/mm^2$). This radical change in grain size would be expected to produce radical changes in mechanical properties and should be avoided. The recrystallization temperature depends on the amount of prior cold work and for this reason it is not possible to predict from these auxiliary tests at what temperature the notch root regions would recrystallize. For this reason, the notch root regions of representative specimens used in the stress relief experiments were examined metallographically to guard against recrystallization or other changes. In all the examinations made no microstructural changes were observed.

Direct Correlation of Residual Stress and Temperature Change

This group of experiments was designed to directly show the correlation between measured residual stress and notch root temperature change. Residual stresses were determined by the hole drilling methods of Soete and Vancrombrugge.[63] Before discussing this correlation it is important to understand the limitations of the hole drilling method.

The hole drilling method is based on measuring the strain produced when residual stresses are relieved by drilling a hole. This method relies on a number of assumptions which are not strictly applicable to this test. The assumptions that are least adhered to in this case are:

1. The plate is infinite compared to the size of the hole. In this test the hole was 1.59 mm in diameter located 4.71 mm from the notch root. This assumption is not seriously violated in that the hole is over three diameters from the free edge.

2. The residual stress does not vary through the thickness.

3. The direction of the principal stresses are known. The principal directions are assumed to be horizontal and vertical.

Four specimens were loaded for ten cycles as in all other tests. Each specimen was subjected to a different stress relief heat treatment designed to produce different amounts of residual stress relief. The heat treatments used were respectively; no heat treatment, heat treatment for 1 hour at 260 C, 1 hour at 465 C and 1 hour at 650 C. The residual stress level was then determined

for each specimen by hole drilling. Nominally identical specimens were subjected to the same loading and heat treatments and their notch root stress-strain response determined in a second round of mechanical testing. In Fig. 17 the percent restoration of the first cycle notch root temperature response vs. the residual stress level measured in nominally identical specimens is plotted. The data forms a straight line. The solid line in the figure was fit by least squares. The degree to which the data fits the straight line is remarkable considering the experimental scatter that will be apparent in similar data shown later. This figure provides strong evidence that residual stress level is correlated with notch root temperature response. It is worth noting that the linear relationship between residual stress level and percent restoration is in agreement with the theoretical results of Rice.[61] This correlation can be used to get estimates of residual stress levels from temperature data.

In summary, the key assumption in claiming a correlation between measured percent restoration and residual stress is that no large mechanical property changes take place. The experiments performed support the validity of this assumption. Other experiments show that there is a good linear correlation between residual

stress level and the percent restoration. This not only directly supports the premise upon which the temperature based assessment of residual stress is based but also suggests that the theoretical results of Rice are reasonable for this geometry.

SECTION VII

SUMMARY OF MAJOR FINDINGS

1. A temperature measuring system which is capable of measuring temperature changes smaller than 0.1 C occurring in times shorter than 0.01 s can be built using thermocouples welded directly to the specimen.

2. A quantitative relationship between temperature change and mechanical variables was described (Eq. (5)) and shown to be valid for purely elastic deformation, purely plastic deformation and strain hardening stress-strain behavior combining both elastic and plastic deformation. The accuracy of the equation was generally better than 10%.

3. Three methods of distinguishing elastic from plastic deformation were proposed and experimentally demonstrated. These three methods supply the following types of information:

(A) Round trip method

(a) Detects plastic deformation. For mild steel, plastic strains as small as 0.0003 were detected.

(b) Determines values for specific plastic work.

(B) The sign method

(a) Determines approximate values of volume dilatation for the elastic portion of deformation; from which pressure may be determined.

(b) Detects plastic deformation. For mild steel, plastic strains as small as 0.002 were detected.

(c) Determines approximate values of specific plastic work at any time during the cycle.

(C) The magnitude method

(a) Detects the presence of plastic deformation. For uniaxial single load cycles in mild steel, plastic strains as small as 0.01 were detected.

4. The first two methods described in item three were applied to the determination of plastic zone size. For the particular edge notched specimens (see Fig. 1) tested this determination was not successful possibly because:

A. The zone was narrow and often missed the thermocouples

B. The zone was made up of many very narrow deformation bands that lost the heat produced by plastic deformation too rapidly to be detected.

5. Results based on the elastic stress distribution of a finite width plate with a circular center hole suggest that identifying areas of plastic deformation as areas in which the axial strain exceeds the uniaxial yield strain may result in large errors when estimating plastic zone size.

6. Comparison of the plastic zone size predicted for the elastic stress distribution with the plastic zone size determined from temperature based stress analysis for finite width plates with circular center holes shows that for this geometry temperature based stress analysis gives plastic zone sizes that are approximately correct.

7. The results of stress relief experiments suggest that the large difference between the notch root stress-strain response on the first cycle and all other cycles was mainly due to the residual stresses created on the first cycle.

8. When overloaded notched members were stress relieved the magnitude of the notch root heating resulting from reloading was partially restored to the value characteristic of the virgin specimen. Data for mild steel showed that the degree of restoration computed as a percentage (see section 6.2) is approximately equal to the percentage of the residual stress removed by the stress relief heat treatment used.

SECTION VIII

CONCLUSIONS

A useful technique of stress analysis based on temperature data has been demonstrated. The single most important capability of this method is its ability to distinguish plastic from elastic deformation. The method has the additional advantages of being a nondestructive, real time method for which the detector life under cyclic loading usually exceeds the specimen life.

Quantitative stress analysis from temperature data is only possible if the temperature data used does not include changes due to conduction. The temperature based stress analysis system developed in this thesis uses a temperature measuring system which is fast enough to collect adiabatic temperature data. This temperature measurement system based on thermocouples welded directly to the specimen was found to be both fast enough and sensitive enough to measure the necessary temperature. An equation that was synthesized from known physics was experimentally demonstrated to be capable of relating measured temperatures to mechanical variables. In experiments on the determination of plastic zone size it was concluded that for the specimens with sharp edge notches temperature based stress analysis utilizing thermocouples was not successful but for a plate with a center hole the technique was successful.

The experiments of this thesis suggest one additional conclusion not directly related to temperature based stress analysis. First, that the large difference between the notch root stress-strain response on the first cycle and all others is largely due to the residual stresses created on the first cycle.

The work presented establishes a basis for temperature based stress analysis. Two of perhaps many potential applications were explored. The thermocouple system used to demonstrate the method is not necessarily the ultimate measurement system but rather a sensible system to use in demonstrating the temperature based stress analysis. The employment of other better temperature measuring systems either existing or those yet to be developed can only expand and improve the capabilities of the method.

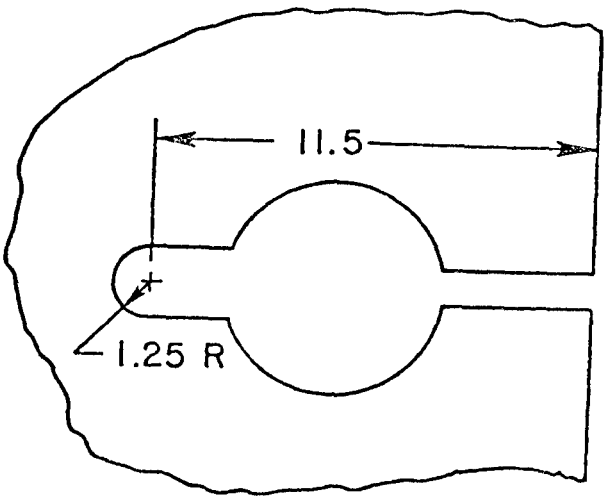

Fig. 1. Notch Root Geometry.

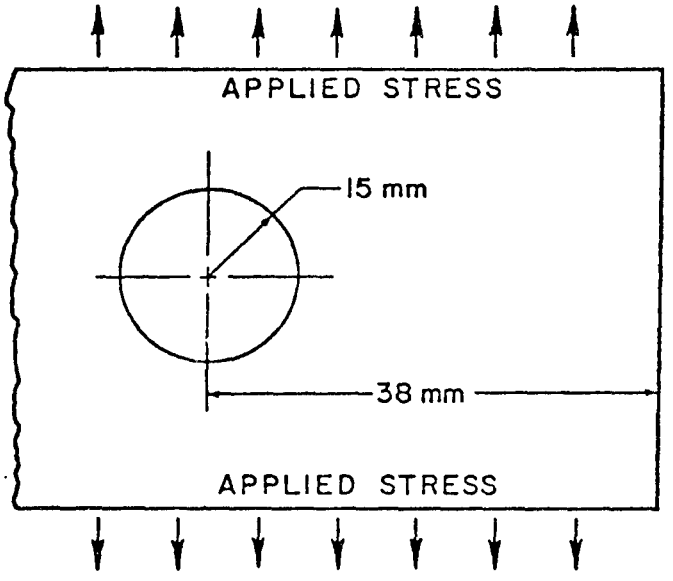

Fig. 2 Plate with a Center Hole.

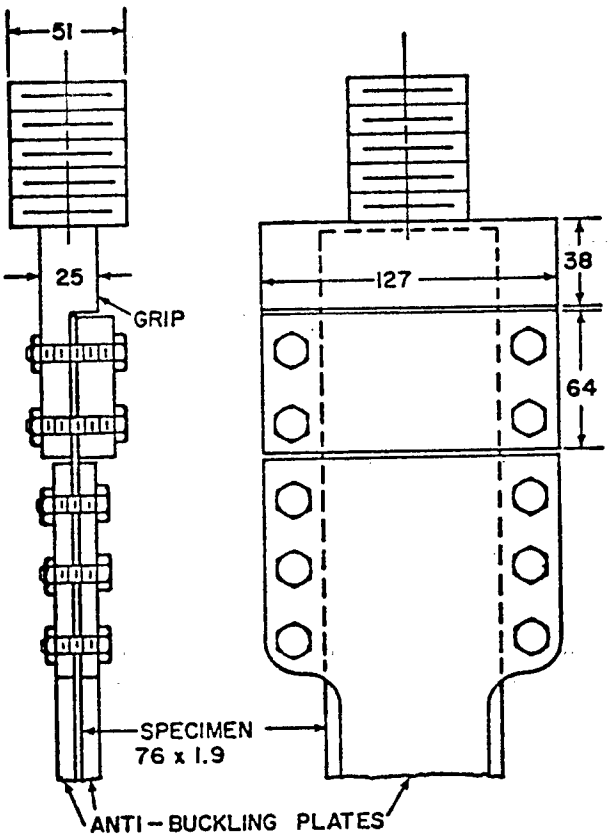

Fig. 3. Grips and Guide Plates for Reversed Cyclic Tests.

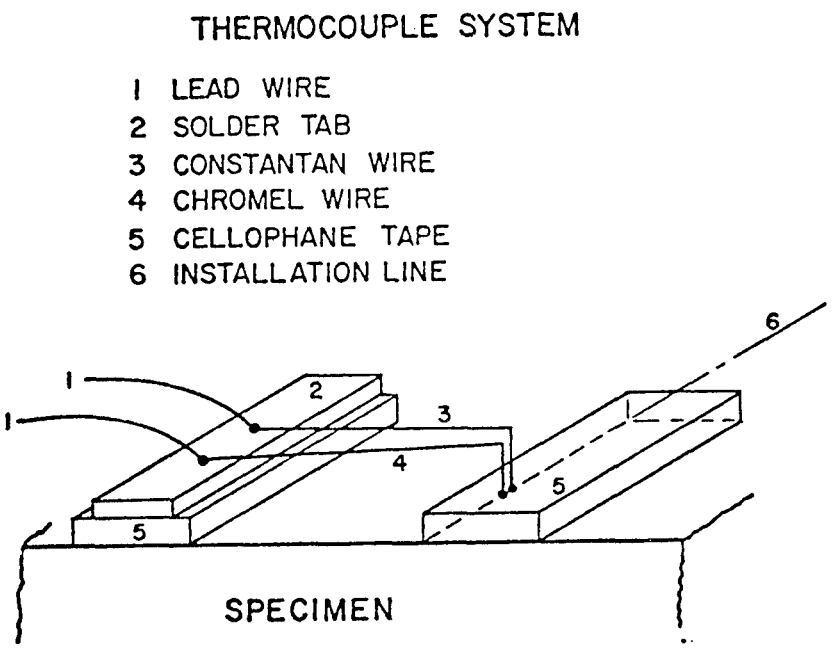

Fig. 4. An Installed Thermocouple.

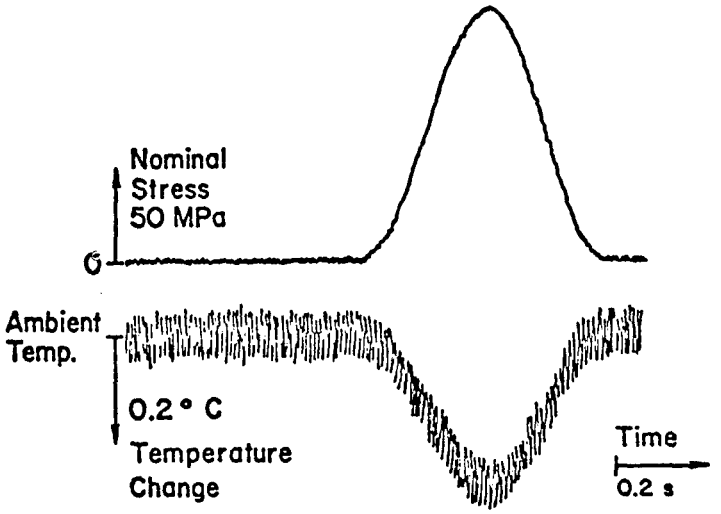

Fig. 5. Temperature Change Caused by Elastic Deformation.

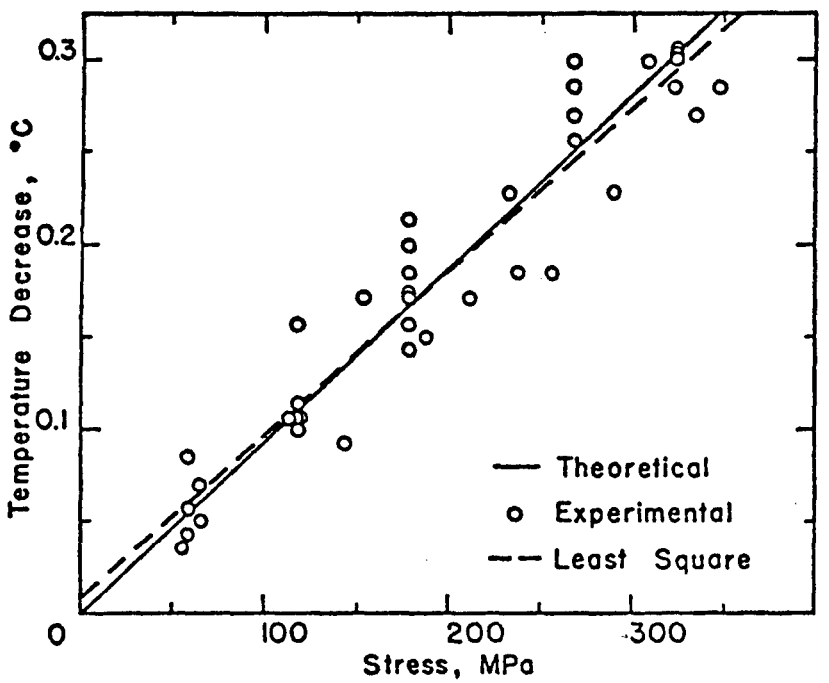

Fig. 6. Temperature Change Caused by Elastic Deformation vs. Stress.

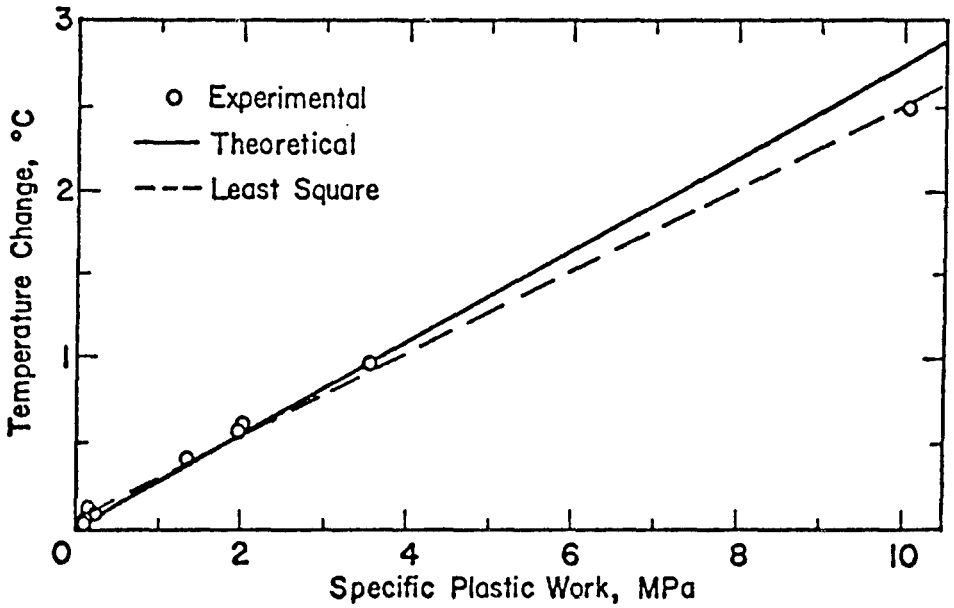

Fig. 7. Temperature Change Caused by Plastic Deformation vs. Specific Plastic Work.

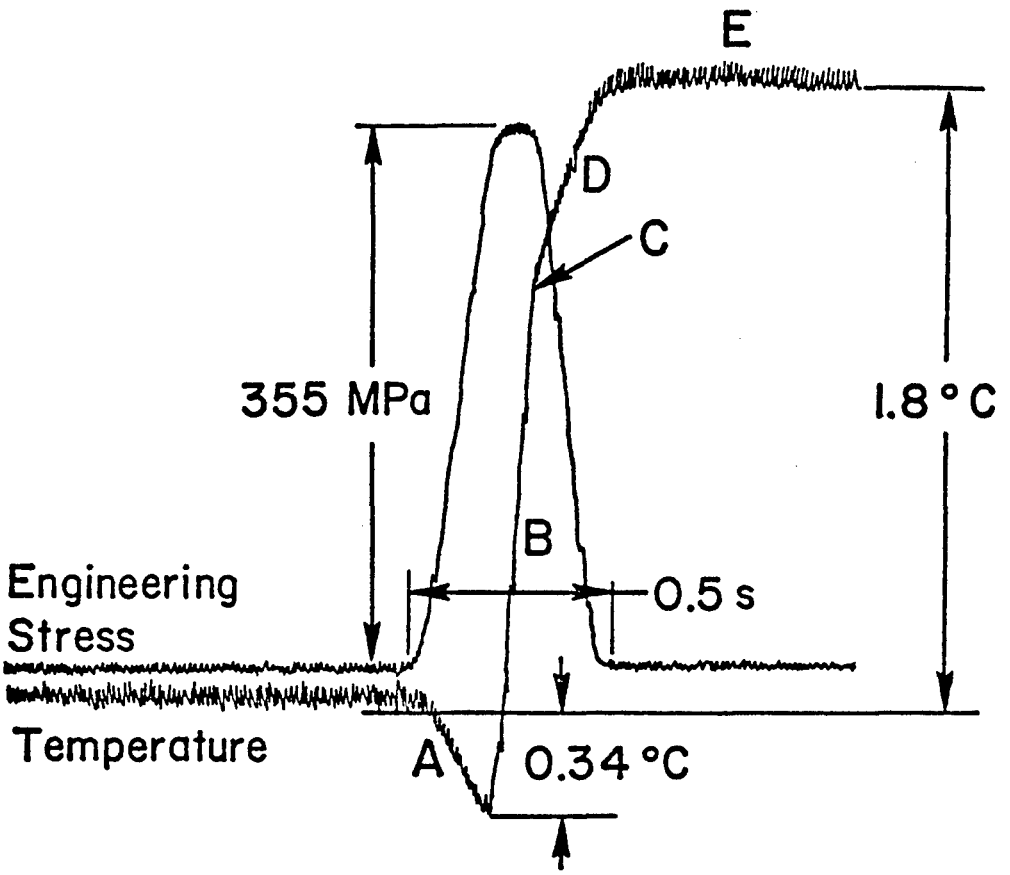

A Loading - Elastic Cooling

B Plastic Heating

C End of Plastic Heating

D Unloading–Elastic Heating

E Steady State After Load Cycle

Fig. 8. Temperature Change Caused by Elastic-Plastic Deformation.

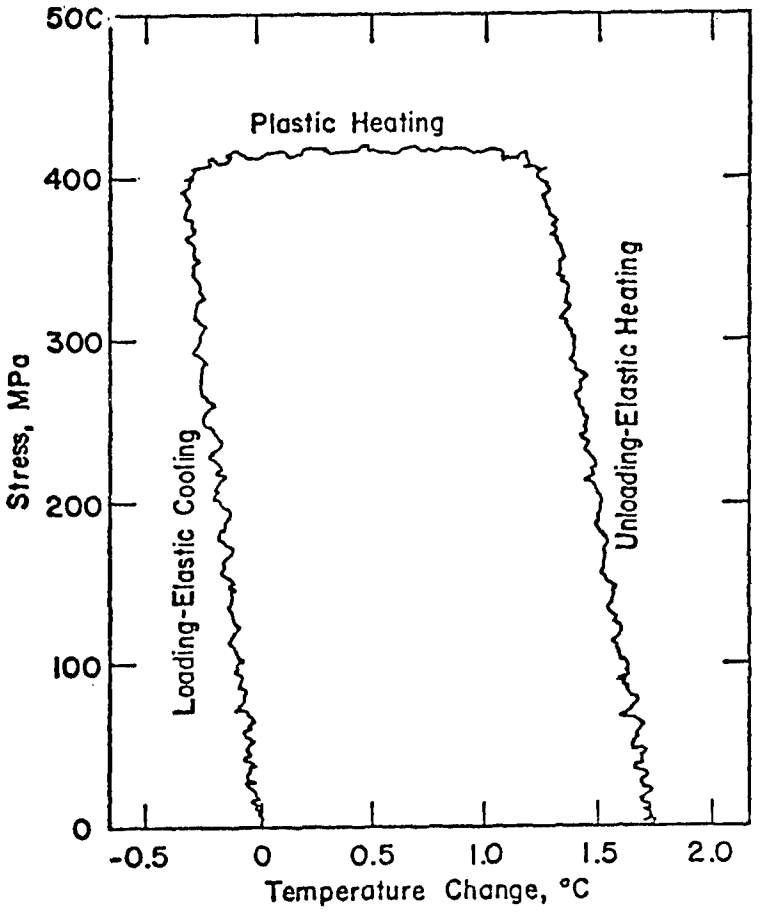

Fig. 9. Stress vs. Temperature Change for the Load Cycle of Fig. 8.

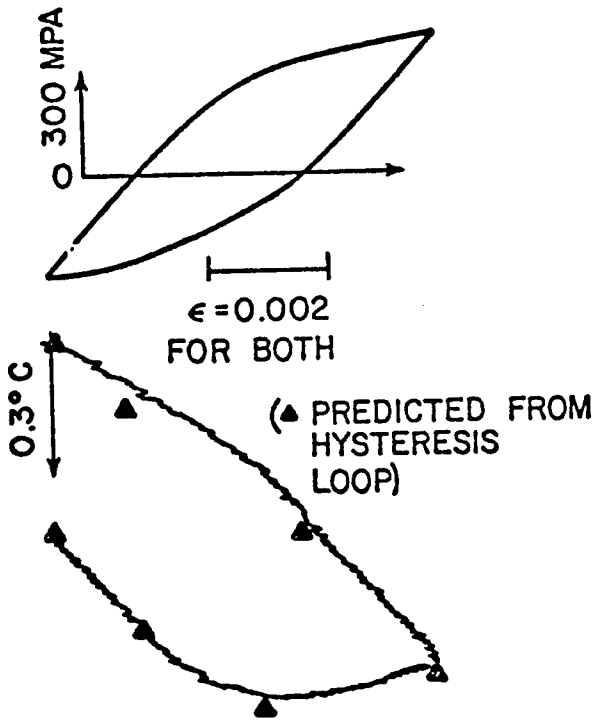

Fig. 10. Temperature Change Caused by Reversed Cyclic Loading.

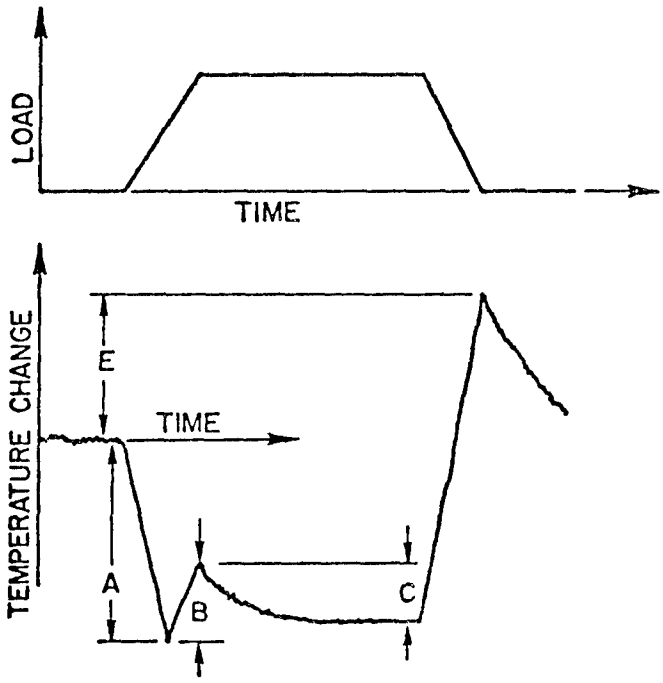

A: ELASTIC COOLING

B: HEATING FROM TENSILE PLASTIC FLOW

(E-C): TOTAL HEATING = SPECIFIC PLASTIC WORK PER CYCLE

NOTE: C IS DUE TO CONDUCTION

Fig. 11. Values Extracted from Time Temperature Plots.

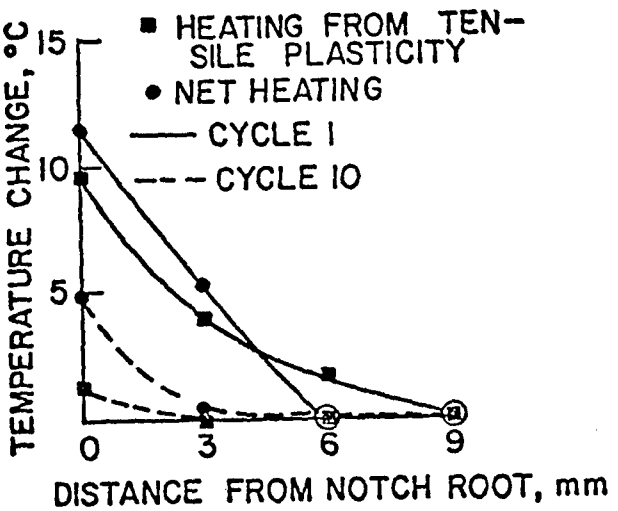

Fig. 12. Temperature Change vs. Distance from Notch Root.

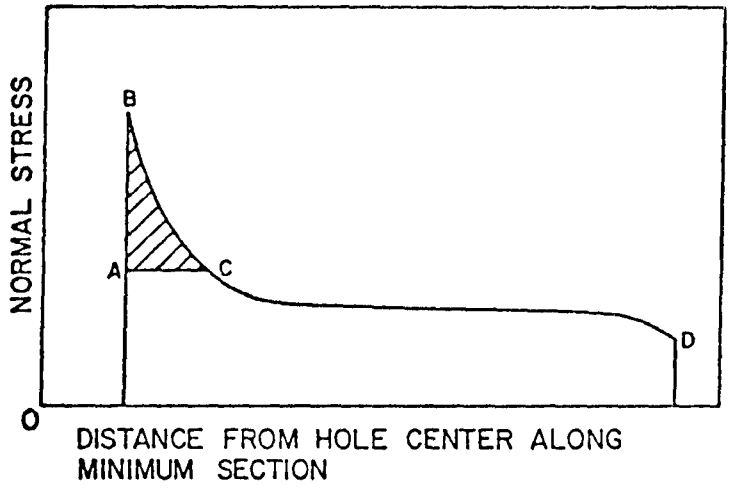

Fig. 13. Assumed Stress Distribution in a Plate with a Hole.

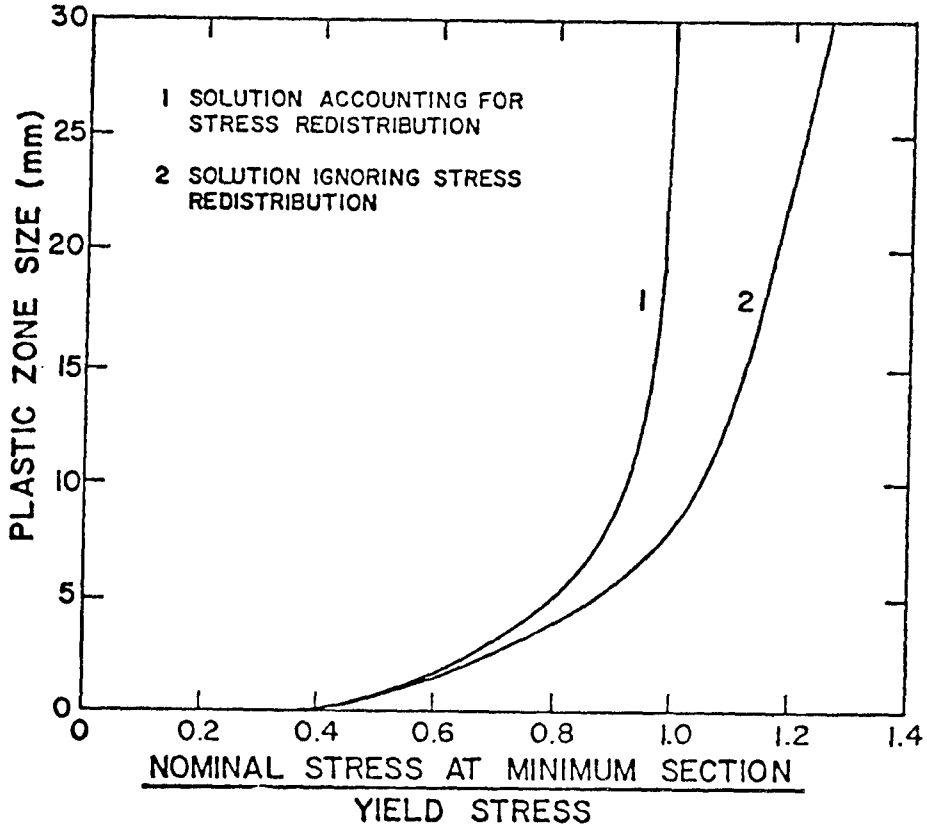

Fig. 14. Theoretical Values of Plastic Zone Size vs. Applied Stress.

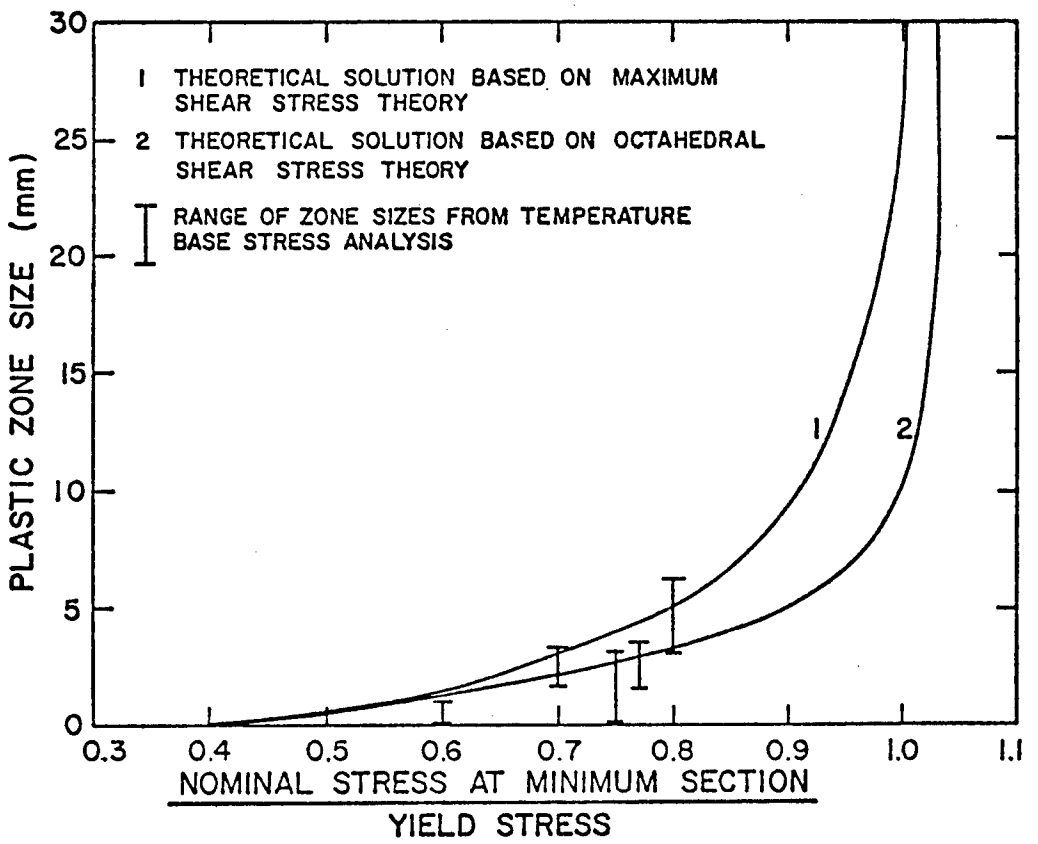

Fig. 15. Theoretically and Experimentally Determined Plastic Zone Sizes.

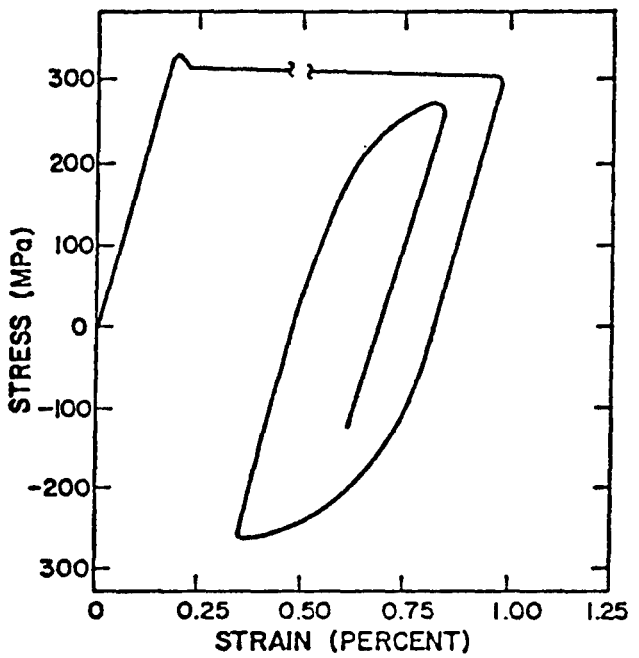

Fig. 16. Monotonic and Cyclic Stress-Strain Behavior of Mild Steel.

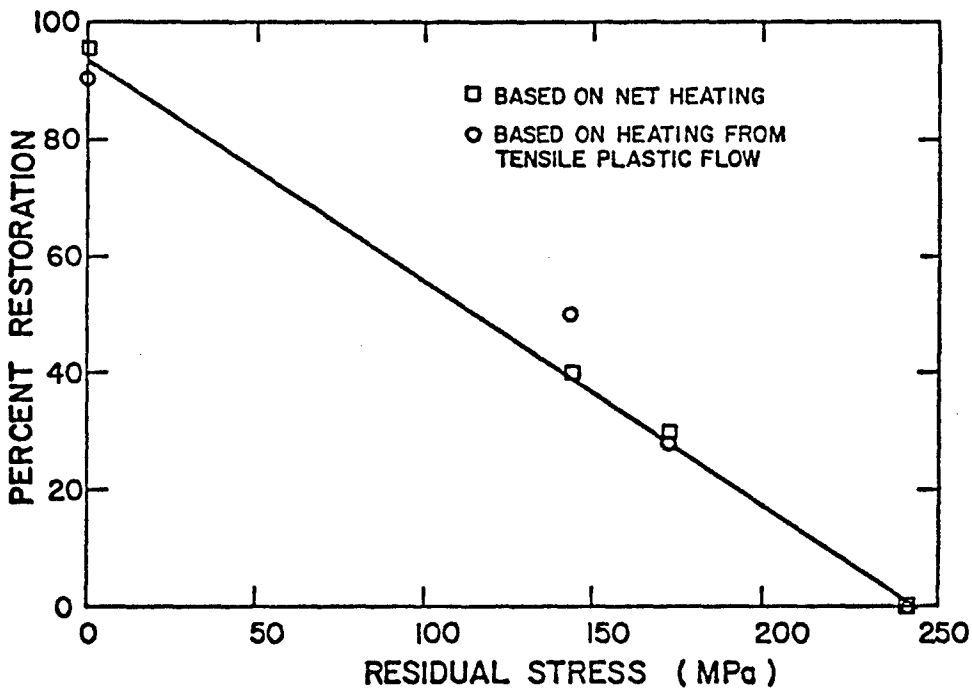

Fig. 17. Percent Restoration vs. Residual Stress.

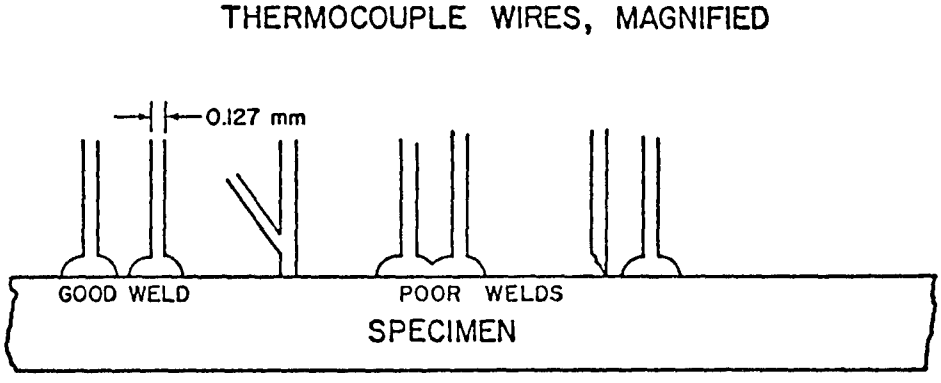

Fig. 18. Examples of a Good Weld and Three Defective Welds.

Table 1--Heat Treatments and Mechanical Properties in 14 Gauge

Heat Treatment No.	Heat Treatment Used	Yield Strength (MPa)	Average Yield Strength (MPa)
1	as received	304 310	307
5	2.5 hour at 881 C in cast iron chips	167 182 181 176	177
6	1 hour at 556 C in cast iron chips	293 318 310	307
6a	1 hour at 685 C in cast iron chips	- - -	-
7	1 hour at 650 C in argon	303 313 298 295 300	302
8	1 hour at 650 C in argon	295 304	300
9	1 hour at 650 C in air	- -	-
average of 6,6a,7,8	heat treated		304

Table 2--Stress Determination by the Sign Method

σ_L,[a] MPa	σ_T,[b] MPa	PERCENT ERROR $100\left(\frac{\sigma_T-\sigma_L}{\sigma_L}\right)$
310	390	12.4
313	302	3.6
343	310	9.8
359	324	9.6
364	363	0.5
364	385	5.6
364	363	0.5
364	377	3.6
370	385	3.8
370	385	3.8
		5.16 Average

a-stress determined from load.

b-stress determined from temperature.

Table 3--Specific Plastic Work Determination by Sign Method

W_s,[a] MPa	W_t,[b] MPa	PERCENT ERROR $100\left(\frac{W_t - W_s}{W_s}\right)$
2.03	1.81	-10
2.97	2.64	-11
3.63	3.31	-14
10.0	8.54	-15
		-12.5 Average

a-specific plastic work determined from stress-strain data.

b-specific work determined from temperature data.

Table 4--Material Properties

Material	E = (MPa)	k' (MPa)	μ	N'	$\alpha \frac{M}{M-CO}$
SAE 1015 80 6hN	2.06x10	944	0.27	0.22	$11.7x10^6$
SAE 1045 410 BHN	2.06x10	2308	0.27	0.146	$11.7x10^6$
Aluminum 2024-T351	$7.3x10^4$	655	0.33	0.065	$23.04x0^6$
Aluminum 7075-T6	$7.3x10^4$	--	0.33	0.146	23.040^6

E = elastic modulus

k' = cyclic strength coefficient

μ = Poisson ratio

α = coefficient of thermal expansion

Table 5--Theoretical Values of Percent Error and Minimum Detectable Strains

Material	Smallest Detectable Plastic Strain	Percent Error E_1	Percent Error E_2
SAE 1015 80 BhN Calculated	7.55×10^{-4}	-18.0	-12.2
SAE 1045 410 BhN Calculated	5×10^{-4}	-12.7	11.9
Aluminum 2026-T751 Calculated	4.4×10^{-4}	- 6.0	3.3
Aluminum 7075-T6 Calculated	9.9×10^{-4}		
A37 Mild Steel Measured	1.4×10^{-3}	-19.7	27

E_1 = Error in estimating the stress corresponding to the minimum temperature which results from assuming ideally elastic stress-strain behavior for a material that strain hardens.

E_2 = Error from estimating the plastic strain when the plastic strain equals .01 m/m which results from assuming ideal elastic-plastic stress-strain behavior for a material that strain hardens.

Table 6 - Effect of Stress Relief on Heating from Tensile Plastic Flow at the Notch.

Heat Treatment Used	Larson-Miller Parameter	ΔT_{1V} (C)	ΔT_{10V} (C)	ΔT_{1S} (C)	ΔT_{10S} (C)	$P = \frac{\Delta T_{1S} - \Delta T_{10S}}{\Delta T_{1V} - \Delta T_{10V}}$
0.1 hr. 575 C	29.0	0.79	0.10	0.10	0.03	0.10
0.1 hr. 613 C	30.3	0.82	0.16	--	--	--
0.1 hr. 650 C	31.5	0.69	0.12	0.58	0.16	0.69
1.0 hr. 150 C	15.2	0.86	0.16	0.16	0.00	0.24
1.0 hr. 260 C	19.2	0.86	0.16	0.26	0.07	0.29
1.0 hr. 465 C	26.5	0.86	0.13	0.43	0.10	0.45
1.0 hr. 575 C	30.6	0.86	0.16	0.56	0.07	0.71
1.0 hr. 601 C	31.4	0.89	0.12	0.40	0.12	0.41
1.0 hr. 650 C	33.2	0.86	0.13	0.86	0.20	0.91
1.0 hr. 660 C	33.6	0.79	0.10	0.79	0.10	1.00
1.0 hr. 660 C	33.6	0.79	0.16	0.66	0.10	0.89
10.0 hr. 260 C	20.2	0.76	0.10	0.23	0.03	0.03
10.0 hr. 448 C	27.3	0.82	0.20	0.56	0.13	0.68
10.0 hr. 601 C	33.0	0.89	0.12	0.79	0.13	0.85
100.0 hr. 575 C	33.6	0.79	0.16	0.74	0.13	0.97
100.0 hr. 472 C	29.5	0.79	0.10	0.56	0.12	0.64
100.0 hr. 260 C	21.1	0.82	0.16	0.29	0.08	0.34

ΔT_{1V} = temperature change on the first load cycle of the virgin specimen.

ΔT_{10V} = temperature change on the tenth load cycle of the virgin specimen.

ΔT_{1S} = temperature change on the first cycle following stress relief.

ΔT_{10S} = temperature change on the tenth cycle following stress relief.

PR = percent recovery.

Table 7 - Effect of Stress Relief on Net Heating at the Notch.

Heat Treatment Used	Larson-Miller Parameter	ΔT_{1V} (C)	ΔT_{10V} (C)	ΔT_{1S} (C)	ΔT_{10S} (C)	$P = \frac{\Delta T_{1S} - \Delta T_{10S}}{\Delta T_{1V} - \Delta T_{10V}}$
0.1 hr. 575 C	29.0	1.19	0.53	0.54	0.54	0.00
0.1 hr. 613 C	30.3	1.28	.61	0.66	0.49	0.24
0.1 hr. 650 C	31.5	1.05	0.56	0.79	0.53	0.53
1.0 hr. 150 C	15.2	1.17	0.58	0.33	0.31	0.03
1.0 hr. 260 C	19.2	1.17	0.58	0.63	0.46	0.28
1.0 hr. 465 C	26.5	1.15	0.53	0.72	0.46	0.42
1.0 hr. 575 C	30.6	1.17	0.58	0.79	0.48	0.53
1.0 hr. 601 C	31.4	1.20	0.54	0.85	0.51	0.29
1.0 hr. 650 C	33.2	1.15	0.53	1.15	0.56	0.95
1.0 hr. 660 C	33.6	1.19	0.53	0.19	0.53	1.00
1.0 hr. 660 C	33.6	1.09	0.56	1.09	0.53	1.06
10.0 hr. 260 C	20.2	1.05	0.49	0.56	0.36	0.35
10.0 hr. 448 C	27.3	1.17	0.59	0.99	0.56	0.74
10.0 hr. 601 C	33.0	1.20	0.54	1.07	0.59	0.93
100.0 hr. 260 C	21.1	1.28	0.61	0.68	0.51	0.15
100.0 hr. 472 C	29.5	1.19	0.53	0.96	0.51	0.69
100.0 hr. 575 C	33.6	1.09	0.56	1.14	0.62	1.00

ΔT_{1V} = temperature change on the first load cycle of the virgin specimen.

ΔT_{10V} = temperature change on the tenth load cycle of the virgin specimen.

ΔT_{1S} = temperature change on the first cycle following stress relief.

ΔT_{10S} = temperature change on the tenth cycle following stress relief.

PR = percent recovery.

APPENDIX I

A. THE THERMOCOUPLE SYSTEM

The purpose of this section is to describe in detail the method of utilizing thermocouples that has evolved through trial and error over the past three years. Two methods that were tried and abandoned will be mentioned to prevent the repetition of past errors by those wishing to improve the present system.

The first unsuccessful system utilized beaded thermocouples. In the earliest experiments the measuring junction was pressed against the specimen surface while in later experiments the measuring junction was welded to the surface. No useful data was ever obtained using either technique. Apparently the response of beaded thermocouples is too slow to pick up the transient temperatures produced by mechanical deformation. If for some reason one desired to use beaded thermocouples, improvements in response time would be expected from using smaller wire sizes (the smallest used in this work were 0.08 mm diameter) or from flattening the measuring junction to increase the contact area.

The second unsuccessful temperature measuring system was based on a thermocouple pair consisting of a single

constantan wire and the steel specimen itself. It was hoped that a single wire system would have the following advantages compared to the two wire systems: faster response, better spatial resolution due to smaller size, and easier installation needing only one weld and one solder junction. Unfortunately, this system had two major problems: first, a method had to be developed to calibrate the thermocouple pair involving a steel specimen of unknown chemical composition and homogeneity; and second, the lead wire configuration of this system enclosed a large area (many sq cm.) which resulted in currents being induced by any changing magnetic field in the vicinity of the specimen. This second disadvantage made this temperature measuring system unworkable.

The signals induced in the single wire system were in phase with the load and were mistaken for temperature changes. An investigation of these signals was conducted when it was observed that temperature changes measured on opposite sides of the same specimen were of opposite sign. The investigation showed that signals were being induced by deformation produced magnetic flux changes caused by the inverse of magnetostriction.[64] A Gaussmeter was used to measure the magnetic flux changes confirming that there were deformation produced flux changes.

Because the induced flux changes are an inherent part of the physics of the deformation of steels the single wire system was abandoned.

The thermocouple system used for all the experiments of this thesis was designed specifically to overcome the problems of the previous two systems. This system (see Fig. 4) utilizes two .13 mm diameter wires of dissimilar metals welded individually to the surface of the specimen. The two wires are welded very close together. This thermocouple based temperature measurement system has the following outstanding features.

1. Commercially available standard thermocouple wire pairs were used. The known relationship between thermocouple output and temperature for standard thermocouple pairs may be used if it is assumed that the two wire ends (.1 mm apart) are at the same temperature.

2. The lead wire configuration of this system makes the area enclosed by the conductors very small, thus eliminating all measurable magnetically induced signals.

3. The reference junction is on a solder tab near the measuring junction (see Fig. 4). Slow changes in room temperature will not produce differences in temperature between the measuring junction and the reference junction

and therefore will not produce annoying changes in apparent temperature.

4. The measuring junction can be precisely positioned by using celophane tape to guide the positioning of the welds.

5. The measuring junction can be easily inspected during testing.

6. As many as one thermocouple per 0.3 mm can be installed. This thermocouple system successfully overcomes the defects of the two earlier systems.

B. THERMOCOUPLE INSTALLATION PROCEDURE

1. Sand off all millscale along the installation line and clean several times with tricloroethane to remove grease. Without thorough cleaning the weld quality will be poor.

2. Solder a 25 mm piece of each type of thermocouple wire to separate wires of a strain gage hook up wire pairs.

3. Carefully lay a piece of celophane tape parallel to and one wire radius away from the line upon which the thermocouples will be installed. This tape provides a base line to work from. Two pieces of tape can be put down, one on each side of the desired installation line making it impossible to weld the thermocouples off the

line. Experience has shown that one piece of tape is usually sufficient.

4. Tape down the lead wire-thermocouple-solder tab unit in the desired location putting tape both underneath and on top of the solder tab to prevent short circuits. Solder tabs may be glued down and new wires made up each time. However, because connecting lead wires to thermocouples wires is time consuming such a procedure is inefficient.

5. Lay a ruler along the installation line to position the thermocouples.

6. Using a low (7x) power binocular microscope bend the wires so that the wires are not touching the specimen and such that when they are forced to the specimen surface they are in the desired location. This usually takes about half of the time needed for a given installation. This bending is done primarily using needlenosed tweezers.

7. The welding of the thermocouple to the specimen is accomplished by touching each thermocouple wire individually to the specimen, short circuiting a 2500 UF capacitor charged to 20 v. Connect one side of the capacitor to a lead wire and the other side of the capacitor to the specimen. Connect a power supply to the capacitor and charge it to 20 volts. Disconnect the

power supply from the capacitor. Press the thermocouple wire down in the desired location striking an arc and producing a weld. Repeat step 7 for all wires. Caution: failure to disconnect the power supply from the capacitor before pressing the wire down shorts the power supply through the wire and burns up the wire.

7a. The strength of the welds depends upon the rate of discharge of the capacitor and the total energy in that discharge. The proper total energy for welding was determined by testing various combinations of voltage and capacitance. The quality of the welds depends very strongly on the rate of discharge of the capacitor which is dependent on both the capacitance and the resistance. The proper rate of discharge was attained by putting various resistances in series with the capacitor until optimum weld quality was obtained. For the configuration used a 150 mm piece of hook-up wire plus the contact resistance of one banana plug provided the correct resistance.

8. All welds should be inspected carefully before use. Fig. 18 shows the three most common bad welds as well as a good weld. Each weld should be inspected under the microscope from several viewing angles. While viewing

the welds under the microscope gently touch one wire of each pair. If the other wire of the pair moves the weld is defective and should be redone.

APPENDIX II

ELECTRICAL NOISE MINIMIZATION

The purpose of this section is to relate some of the actual practical experience gained in working with the particular thermocouple system used for temperature measurement in this report. No attempt will be made to write a general text on the handling of low level signals because general texts are rapidly available.[65]

At the present time the average peak to peak noise level on the recorded temperature signals is about 2 microvolts without using dummy thermocouples and about 1 microvolt peak to peak when using dummy thermocouples. One microvolt noise is the limit set by the internal noise of the amplifier so that major improvement is possible only with a lower noise amplifier. The amplifier determined noise limit was only recently reached by continual improvement in the layout, grounding, and connection of the thermocouple to the amplifiers. The following is a list of practices that were found to be important in minimizing noise.

1. The use of differential amplifiers is essential. A large voltage fluctuation common to both the positive and negative lead wire occurs with respect to ground in

the thermocouple system used. This fluctuation is referred to as common mode noise. In an ordinary (single ended) amplifier the negative lead is connected to ground and the signal on the positive lead referenced to ground is amplified. The result is that in a single ended amplifier the common mode noise signal is amplified along with the signal. For the thermocouple system used the common mode noise is orders of magnitude larger than the signal. A differential amplifier ideally amplifies the difference in potential between the plus and minus input and is therefore immune to common mode noise. Because the differential amplifier eliminates nearly all common mode noise it makes possible the temperature measurements which were made in this thesis. The common mode rejection of differential amplifiers is degraded by electrical differences in the lead wires so that lead wire pairs should be as identical as possible.

2. The specimen must be grounded or the noise will be overwhelming. Gripping the specimen in the machine appears to provide adequate grounding.

3. Noise can be reduced by reducing the source resistance. For the thermocouple system used substantial noise reduction was obtained by upgrading the weld

quality (see Appendix IB) which reduced source resistance. Use of the largest diameter thermocouple that heat transfer considerations will allow will also reduce source resistance.

4. Noise can be reduced by reducing the inductive, capacitive, and electrostatic pick up in the lead wires. These types of electrical pick up can be reduced as follows.

a. Make lead wires as short as possible.

b. Use specially designed shielded twisted pair cables. Experience showed, however, that in this thermocouple system there was no noticable difference between shielded twisted pair leads, twisted strain gauge wire leads and as received flat bonded strain gauge wire pairs.

c. Lead wires should be immobilized. Large cable motion produces measurable signals.

5. Noise can be reduced greatly by using electronic filters to limit the band width. In this investigation a filter which begins attenuating at 300 Hz was used. This filter attenuation increases by a factor 3dB for each additional decade of frequency. Further improvement should be possible with a filter with attenuation that increases more rapidly with frequency.

6. Noise was reduced by a factor of three by moving the differential amplifiers from on top of, to a few feet away from the light pen ocillograph. This simple change in layout resulted in the single largest noise reduction achieved.

7. The signal to noise ratio can be improved by using the most sensitive thermocouple available (type E).

8. A dummy thermocouple consisting of two wires of the same material can be used to cancel noise. This is done by installing the dummy as close to the actual thermocouple as possible and routing the lead wires of the thermocouple and dummy in as identical manner as possible. The thermocouple and the dummy will have nearly identical noise signals. Both the thermocouple and dummy signals are amplified in separate differential amplifiers. The output of the thermocouple amplifier and dummy amplifier are subtracted from each other in a third differential amplifier. The result is that the noise of the dummy cancels the noise of the thermocouple and the noise is reduced by about a factor of two. This system requires three differential amplifiers per channel and was only used in the experiments of section 3.2.

APPENDIX III

Presented in this appendix is a theoretical analysis of the consequences of using the sign method (see section 4.2) and assumed ideal elastic-plastic stress-strain behavior (flat topped yielding) in interpreting temperature data from tests of power law strain hardening materials. Specifically, the minimum detectable plastic strain, the error in estimating the stress corresponding to the minimum temperature, and the error in estimating plastic strain from temperature changes which follow the minimum temperature are derived. The minimum detectable plastic strain is the plastic strain corresponding to the minimum temperature. The starting point for these derivations are the uniaxial forms of Eq. (5b) and Eq. (7).

$$\Delta\theta = \int \frac{\sigma dE_p}{\rho c} - \frac{\theta\alpha}{\rho c}\sigma \quad \ldots\ldots\ldots\ldots\ldots\ldots\ldots\ldots \quad (5b)$$

$$\varepsilon_p = \left(\frac{\sigma}{K'}\right)^{1/N'} \quad \ldots\ldots\ldots \quad (7a) \quad \text{or} \quad dE_p = \left(\frac{1}{K'}\right)^{\frac{1}{N'}} \frac{1}{N'}\,\sigma^{\left(\frac{1}{N'}-1\right)} \quad \ldots\ldots\ldots \quad (7b)$$

Consider the integral in Eq. (5b),

$$I = \int \frac{\sigma\, E_p}{\rho c}$$

Using Eq. (7a) and the fact that $I = 0$ when $\sigma = 0$ this integral becomes:

$$I = \frac{1}{\rho c(1+N')} \sigma \left(\frac{\sigma}{k'}\right)^{\frac{1}{N}} = \frac{1}{\rho c(1+N')} \sigma\varepsilon_p \quad \ldots\ldots\ldots\ldots \quad (8)$$

The stress at the minimum temperatuer can be found by substituting Eq. (8) into Eq. (5b) and differentiating $\Delta\theta$ with respect to stress and setting the derivative equal to zero.

$$\frac{d\Delta\theta}{d\sigma} = \frac{1}{\rho c}\left[\frac{1}{N'}\left(\frac{\sigma}{k'}\right)^{\frac{1}{N'}} - \theta\alpha\right] = 0 \quad \ldots\ldots\ldots\ldots\ldots\ldots \quad (9)$$

Eliminating stress using Eq. (7) and Eq. (9) and solving for plastic strain the minimum detectable plastic strain is found to be:

$$\varepsilon_{pc} = N'\alpha\theta \quad \ldots\ldots\ldots\ldots\ldots\ldots\ldots\ldots\ldots\ldots\ldots\ldots\ldots\ldots\ldots\ldots (10)$$

Using Eq. (10) and Eq. (7a) the stress at minimum temperature is:

$$\sigma_I = k'(N'\alpha\theta)^{N'}$$

Using Eq. (5b) the minimum temperature is:

$$\Delta\theta_I = I(\sigma_I) - \frac{\alpha\theta}{\rho c}\sigma_I$$

If ideal elastic-plastic behavior is assumed, the stress (σ_A) calculated from temperature data would be:

$$\sigma_A = -\frac{\rho c \Delta\theta_I}{\alpha\theta}$$

The percent error in estimating stress from the minimum temperature can be derived from the preceding three expressions.

$$E^1 = 100\,\frac{\sigma_A - \sigma_I}{\sigma_I} = -100\,\frac{\varepsilon_{PI}}{\alpha\theta(N'+1)} \quad \ldots\ldots\ldots\ldots \quad (11)$$

If ideal elastic-plastic stress-strain behavior is assumed, the plastic strain (ε_{PA}) that would be estimated from the temperature increase which follows the minimum temperature would be

$$\sigma_I\,\varepsilon_{PA} = (\Delta\theta - \Delta\theta_I)\rho c$$

The percent error E2 in this estimated plastic strain can be found using Eqs. (5b), (8) and (11)

$$E2 = 100\,\frac{\varepsilon_{PA} - \varepsilon_P}{\varepsilon_P}$$

$$E2 = \frac{\left(\frac{1}{N'+1}\right)(\varepsilon_p\sigma - \varepsilon_{PI}\sigma_I) - \theta\alpha(\sigma - \sigma_I) - \varepsilon_P\sigma_I}{\varepsilon_P\,\sigma_I} \quad \ldots. \quad (12)$$

References

1. Yokobori, T., Sato, K. and Yaguchi, H., "Observations of Microscopic Plastic Zones and Slip Band Zone at the Tip of a Fatigue Crack," Reports of the Research Institute for Strength and Fracture of Materials, Tohoku University, Sendai, Japan, Vol. 9, No. 1, November 1973, pp. 1-10.

2. Green, A. P. and Hundy, B. D., "Initial Plastic Yielding in Notched Bend Tests," Journal of the Mechanics and Physics of Solids, Vol. 4, pp. 128-144.

3. Saxena, A. and Antolovich, S. D., "Low Cycle Fatigue, Fatigue Crack Propagation and Substructures in a Series of Polycrystalline Cu-Al Alloys," Metallurgical Transactions, Vol. 6a, September 1975, pp. 1809-1928.

4. Hoeppner, D., Danford, V. and Pettit, D. E., "A New Technique for Viewing Deformation Zones at Crack Tips," Experimental Mechanics, Vol. 11, No. 6, June 1971, pp. 280-283.

5. Wilkins, M. A. and Smith, G. C., "Dislocation Structures Near a Propagating Fatigue Crack in an Al/1/2% Mg Alloy," Acta Metallurgica, Vol. 18, September 1970, pp. 1035-1043.

6. Dudderar, T. D. and O'Regan, R., "Measurement of the Strain Field Near a Crack Tip in Polymethylmethacrylate by Holographic Interferometry," Experimental Mechanics, Vol. 11, No. 2, February 1971, pp. 49-56.

7. Gerberich, W. W., "Plastic Strains and Energy Density in Cracked Plates, Part I Experimental Technique and Results," Experimental Mechanics, Vol. 4, No. 11, November 1974, pp. 335-343.

8. Davidson, D. L. and Lankford, J., Jr., "Plastic Strain Distribution at the Tips of Propagating Fatigue Cracks," Journal of Engineering Materials and Technology, Vol. 98, January 1976, pp. 24-29.

9. Taggart, R., Plononis, D. H. and James, L. A., "Plastic-strain Distribution at the Root of a Sharp Notch," Experimental Mechanics, Vol. 7, No. 9, September 1967, pp. 386-391.

10. Underwood, J. H. and Kendall, D. P., "Measurement of Microscopic Plastic-strain Distribution in the Region of a Crack Tip," Experimental Mechanics, Vol. 9, No. 7, July 1969, pp. 296-304.

11. Baxter, W. J., "The Detection of Fatigue Damage by Exoelectron Emission," Journal of Applied Physics, Vol. 44, No. 2, February 1973, pp. 608-614.

12. Thompson, William (Lord Kelvin), "On the Dynamical Theory of Heat," Transcations of the Royal Society of Edinburgh, Vol. 20, 1853, pp. 261-283.

13. Joule, J. P., "On Matter, Living Force and Heat," Manchester "Courier" Newspaper, May 5 and 12, 1847, Joule's Scientific Papers, Vol. 1, Dawson of Pall Mall, 16 Pall Mall, London, S. W.I., 1963, p. 265. Cited by Moss, G. L., "Measurement and Analysis of Thermal Inhomogeneities Developed During the Plastic Deformation of Copper," Ballistic Research Laboratories, Aberdeen Proving Ground, Maryland, 1972 (NTIS AD-756-416), p. 13.

14. Hirin, G. A., "Theorie Mechanique de la Chaleur," Vol. 1, Third Ed., 1875, pp. 95-103, Cited by Ibid.

15. Titchener, A. L. and Bever, M. B., "The Stored Energy of Cold Work," Progress in Metal Physics, Vol. 7, 1958, pp. 247-338.

16. Bever, M. B., Holt, D. and Titchener, A., "The Stored Energy of Cold Work," Progress in Metal Science, Vol. 17, 1973.

17. Moss, G. L., "Measurement and Analysis of Thermal Inhomogeneities Developed During the Plastic Deformation of Copper," Ballistic Research Laboratories, Aberdeen Proving Ground, Maryland, 1972 (NTIS AD-756-416).

18. Nadai, A. and Manjoine, M. J., "High Speed Tension Test at Elevated Temperatures - Parts II and III," Journal Applied Mechanics, Vol. 8, June 1941, pp. A77-A91, Cited by op. cit.

19. Moss, G. L. and Pond, R. B., "Inhomogeneous Thermal Changes in Copper During Plastic Elongation" Metallurtical Transactions A, Vol. 6A, June 1975, pp. 1223-1235.

20. Dillon, O. W., "A Nonlinear Thermoelasticity Theory," Journal of The Mechanics and Physics of Solids, Vol. 10, 1962, pp. 123-131.

21. Dillon, O. W., "An Experimental Study of the Heat Generated During Torsional Oscillations, Ibid, pp. 233-234.

22. Dillon, O. W., "Temperatures Generated in Aluminum Rods Undergoing Torsional Oscillations," Journal of Applied Physics, Vol. 33, No. 10, Oct. 1962, pp. 3100-3105.

23. Dillon, O. W., "Coupled Thermoplasticity," Journal of the Mechanics and Physics of Solids, Vol. 11, No. 1, 1963, pp. 21-33.

24. Dillon, O. W. and Taucher, T. R., "The Experimental Technique for Observing Temperatures Due to the Coupled Thermoelastic Effect," International Journal of Solid Structures, Vol. 2, 1966, pp. 385-391.

25. Franyuk, V. A. and Rantsevitch, V. B., "Investigation into the Energy Dissipated in Carbon Steels in a Fatigue Process," Industrial Laboratory, Vol. 38, No. 12, December 1972, pp. 1898-1900.

26. Montgomery, D., "The Temperature Wave Method of Determining Fracture Toughness Values Due to Crack Propagation" Journal of Materials Science, Vol. 10, 1975, pp. 205-213.

27. Schonert, K. and Weichert, R., "Abhangigkeit von der Ausbreitungsgeschwindigkeit," Chemie Ingenieur Techaid, Vol. 41, March 1966, pp. 295-300.

28. Weichert, R. and Schonert, K., "On the Temperature at the Tip of a Fast Running Crack," Journal of Mechanics and Physics of Solids, Vol. 22, 1974, pp. 127-133.

29. Abdi, A. D., Krane, N. C. and Small, N. C., "Detection of Strain Induced Thermal Signals in Metals," Mechanics Research Communications, Vol. 5, No. 1, 1978, pp. 15-18.

30. Attermo, R. and Ostberg, G., "Measurement of Temperature Rise Ahead of A Fatigue Crack," International Journal of Fracture Mechanics, Vol. 7, 1971, pp. 122-129.

31. Reifsnider, K. L. and Williams, R. S., "Determination of Fatigue-Related Heat Emission in Composite Materials," Experimental Mechanics, Vol. 14, No. 12, December 1974, pp. 479-485.

32. Marcus, L. A. and Stinchomb, W. W., "Measurement of Fatigue Damage in Composite Materials," Experimental Mechanics, Vol. 15, No. 2, February 1975, pp. 55-60.

33. Charles, J. A., Appl, F. J. and Francis, J. E., "Using the Scanning Infrared Camera in Experimental Fatigue Studies," Experimental Mechanics, Vol. 15, No. 4, April 1975, pp. 133-138.

34. Wilburn, D. K., "Temperature Profiles Observed in Tensile Specimens During Physical Test," Proceedings of the Second Biennial Infrared Information Exchange, St. Louis, 1974, pp. 59-65.

35. Peterson, R. E., Stress Concentration Factors, New York, Wiley, 1974, p. 36.

36. Howland, R. C., "On the Stress in the Neighborhood of a Circular Hole in a Strip Under Tension," Transactions of the Royal Society of London, Vol. 229A, January 1930, pp. 49-84.

37. Brueggeman, W. C. and Mayer, M., "Guides for Preventing Buckling in Axial Fatigue of Thin Sheet-Metal Specimens," National Advisory Committee for Aeronautics, Technical Note. No. 931, 1944, pp. 1-7.

38. Kator, L. and Nyuasz, P., Problemi Prochnosti, No. 1, 1971, Kiev.

39. Hertzberg, R. W., "Deformation and Fracture of Engineering Materials," New York, Wiley, 1976.

40. Kfouri, A. P. and Miller, K. J., "Crack Separation Energy Rates in Elastic-Plastic Fracture Mechanics," Proceedings of the Institution of Mechanical Engineers, London, 1976, Vol. 190, No. 48, pp. 571-584.

41. Czoboly, E. and Sandor, B. I., "Fatigue Behavior of Notched Specimens: Engineering Experiment Station Report No. 39, University of Wisconsin, August, 1974.

42. Bathias, C. and Pelloux, "Fatigue Crack Propagation in Martensitic and Austinitic Steels," Metallurgical Transactions, Vol. 4, May 1974, pp. 1265-1273.

43. Pineau, A. G. and Pelloux, R. M., "Influence of Strain-Induced Martinsitic Transformations on Fatigue Crack Growth Rates in Stainless Steels," Metallurgical Transactions, Vol. 5, May 1974, pp. 1103-1112.

44. Hahn, G. T., "Dislocation Etch-Pitting of Iron and Mild Steel," Transactions of the Metallurgical Society of AIME, Vol. 224, April 1962, pp. 395-397.

45. Hahn, G. T. and Sapey, D., "The Etch-Pitting Response of Annealed and Deformed Armco Iron," Transactions of the ASM, Vol. 50, 1966, pp. 16-25.

46. Crussard, C., Borione, R., Plateau, Y. and Maratray, F., "A Study of Impact Tests and the Mechanism of Brittle Fracture," Journal of the Iron and Steel Institute, June 1956, pp. 146-173.

47. Schijve, J., "The Assumulation of Fatigue Damage in Aircraft Materials and Structures," Advisory Group for Aerospace Research and Development, 1972 (AGARD-AG-157).

48. Potter, J. M., "The Effect of Load Interaction and Sequence on the Fatigue Behavior of NOtched Coupons," Cyclic Stress-Strain Behavior. Analysis, Experimentation, and Failure Prediction, ASTM STP 519, American Society for Testing and Materials, 1973, pp. 109-132.

49. Gerber, T. L. and Fuchs, H. O., "Improvement in the Fatigue Strength of Notched Bars by Compressive Self-Stresses," Achievement of High Fatigue Resistance in Metals and Alloys, ASTM STP 467, American Society for Testing and Materials, 1969, pp. 276-295.

50. Crews, J. H., "Crack Initiation at Stress Concentrations as Influenced by Prior Local Plasticity, op. cit., pp. 37-52.

51. Imag, L. A., "Effects of Initial Loads and of Moderately Elevated Temperature on the Room-temperature Fatigue Life of Ri-8Sl-lMo-iV Titanium-allow Sheet," National Aeronautics and Space Administration, (NASA, TN D-4061).

52. Watson, P., Hoddinott, D. S. and Norman, J. P., "Periodic Overloads and Random Fatigue Behavior," Cyclic Stress-Strain Behavior. Analysis, Experimentation, and Failure Prediction, ASTM STP 519, American Society for Testing and Materials, 1973, pp. 271-284.

53. Rowland, E. S., "Effect of Residual Stress on Fatigue," Proceedings, Tenth Sagamore Conference, Syracuse University Press, 1964, pp. 229-244.

54. Impellizzeri, L. F., "Cumulative Damage Analysis in Structural Fatigue," Effects of Environment and Complex Load History on Fatigue Life, ASTM STP 462, American Society for Testing and Materials, 1970, pp. 40-68.

55. Smith, C. R., "Fatigue-service Life Prediction Based on Tests at Constant Stress Level," Proceedings of SESA, Vol. 16, No. 1, 1958, p. 9.

56. Gassner, E., "Ueber bisherige Ergebmisse aus Festigkeitsversuchen im Sinne der Bertriebsstatistik, Lilienthal Gesellschaft fur Luftfahrtforschung," Bericht 106, I. Teil, 1939, Translation NACA Tm 1266, 1950, National Advisory Committee for Aeronautics, TM 1266, 1950, Cited by Schijve, J., "The Accumulation of Fatigue Damage in Aircraft Materials and Structures," Advisory Group for Aerospace Research and Development, 1972 (AGARD-AG-157).

57. Simkins, D. and Neulieb, R. L., "Load-Time Relaxation of Residual Stresses," Journal of Aircraft, Vol. 9, No. 12, December 1972, pp. 867-868.

58. Sandor, B. I., "Metal Fatigue with Elevated Temperature Rest Periods," Achievement of High Fatigue Resistance in Metals and Alloys, ASTM STP 467, American Society for Testing and Materials, 1970, pp. 254-270.

59. Rice, J. R., "Plastic Yielding at a Crack Tip," Proceedings of the First International Conference on Fracture, Sendal, Japan, Vol. 1, September 1965, pp. 283-308.

60. Hult, J. A. and McClintock, "Elastic-Plastic Stress and Strain Distribution Around Sharp Notches Under Repeated Shear," International Congress of Applied Mathematics, Vol. 8, No. 9, 1957, pp. 51-58.

61. Hutchinson, J. W., "Singular Behavior at the End of a Tensile Crack in a Hardening Material," Journal of the Mechanics and Physics of Solids, Vol. 16, 1968 pp. 13-31.

62. Gowda, C. V. B. and Topper, T. H., "Performance of Miniature Resistance Strain Gages in Low-Cycle Fatigue," Experimental Mechanics, Vol. 10, No. 10, January 1970, pp. 27N-38N.

63. Soete, and Vancrombrugge, R., "An Industrial Method for the Determination of Residual Stresses," Proceedings of the SESA, Vol. 8, No. 1, 1950, pp. 17-28.

64. Brown, W. F., "Magnetoelastic Interactions, Berlin, Springer-Verlag, 1966, p. 1.

65. Morrison, R., "Grounding and Shielding Techniques in Instrumentation," New York, John Wiley and Sons, 1977.